

# Journal Pre-proof

Effect of elevated in-service temperature on the mechanical properties and microstructure of particulate-filled epoxy polymers

Mojdeh Mehrinejad Khotbehsara, Allan Manalo, Thiru Aravinthan, Kakarla Raghava Reddy, Wahid Ferdous, Hong Wong, Ali Nazari



PII: S0141-3910(19)30322-2

DOI: <https://doi.org/10.1016/j.polymdegradstab.2019.108994>

Reference: PDST 108994

To appear in: *Polymer Degradation and Stability*

Received Date: 18 May 2019

Revised Date: 1 September 2019

Accepted Date: 3 October 2019

Please cite this article as: Khotbehsara MM, Manalo A, Aravinthan T, Reddy KR, Ferdous W, Wong H, Nazari A, Effect of elevated in-service temperature on the mechanical properties and microstructure of particulate-filled epoxy polymers, *Polymer Degradation and Stability* (2019), doi: <https://doi.org/10.1016/j.polymdegradstab.2019.108994>.

This is a PDF file of an article that has undergone enhancements after acceptance, such as the addition of a cover page and metadata, and formatting for readability, but it is not yet the definitive version of record. This version will undergo additional copyediting, typesetting and review before it is published in its final form, but we are providing this version to give early visibility of the article. Please note that, during the production process, errors may be discovered which could affect the content, and all legal disclaimers that apply to the journal pertain.

© 2019 Published by Elsevier Ltd.

# 1 **Effect of elevated in-service temperature on the mechanical properties and** 2 **microstructure of particulate-filled epoxy polymers**

3 Mojdeh Mehrinejad Khotbehsara<sup>1</sup>, Allan Manalo<sup>1</sup>, Thiru Aravinthan<sup>1</sup>, Kakarla Raghava  
4 Reddy<sup>1</sup>, Wahid Ferdous<sup>1</sup>, Hong Wong<sup>2</sup>, and Ali Nazari<sup>3</sup>

## 5 **Abstract**

6 In civil engineering applications, epoxy-based polymers are subject to different  
7 environmental conditions including in-service temperature, which might accelerate their  
8 degradation and limit their application ranges. Recently, different particulate fillers were  
9 introduced to enhance the mechanical properties and reduce the cost of epoxy-based  
10 polymers. This paper addresses the effect of in-service elevated temperature (from room  
11 temperature to 80°C) in particulate-filled epoxy based resin containing up to 60% by volume  
12 of fire retardant and fly ash fillers through a deep understanding of the microstructure and  
13 analysis of their mechanistic response. An improvement in the retention of mechanical  
14 properties at in-service elevated temperature was achieved by increasing the percentages of  
15 fillers. The retention of compressive and split tensile strength at 80°C for the mix containing  
16 60% fillers was 72% and 52%, respectively, which was significantly higher than the neat  
17 epoxy. Thermo-dynamic analysis showed an increase in glass transition temperature with the  
18 inclusion of fillers, while these mixes also experienced less weight loss compared to neat  
19 epoxy, indicating better thermal stability. Scanning electron microscopy images showed the  
20 formation of dense microstructures for particulate-filled epoxy based resin at elevated  
21 temperatures. This indicates that the particulate filled epoxy resin exhibits better engineering

---

<sup>1</sup>Centre for Future Materials (CFM), School of Civil Engineering and Surveying, University of Southern Queensland, Toowoomba, QLD 4350, Australia.

<sup>2</sup> Imperial College London, Department of Civil and Environmental Engineering, Kensington, London SW7 2AZ, UK

<sup>3</sup>Centre for Sustainable Infrastructure, Faculty of Science, Engineering and Technology, Swinburne University of Technology, Hawthorn, Victoria 3122, Australia

22 properties at in-service elevated temperatures, increasing their durability and therefore their  
23 suitability for civil engineering applications. A simplified prediction equation based on power  
24 function was proposed and showed a strong correlation to the experimental compressive and  
25 splitting tensile strength at different levels of in-service elevated temperature.

26 **Keywords:** Epoxy resin; particulate fillers; in-service elevated temperature; mechanical  
27 properties; microstructure; prediction model.

28

## 29 1. Introduction

30 Epoxy resins are now commonly used as matrices in fibre reinforced polymer (FRP)  
31 composites as well as in coating, binding and adhesive materials [1-2]. This thermosetting  
32 resin is used for pavement overlays, wastewater pipes, hazardous waste containers, and  
33 decorative construction panels in aggressive environmental conditions [3-9]. They are also  
34 used as infill for structural repair systems [6,10,11] due to their superior properties including  
35 modulus and strain, tensile strength, strength development, resistance to chemical attacks and  
36 drying shrinkage compared to ordinary Portland cement-based materials. Recent examples of  
37 structural applications of epoxy resins include as grout in the annulus between damaged pipe  
38 and outer FRP repair systems in underground and underwater pipelines [12], as infill material  
39 for pre-fabricated FRP jackets for damaged columns [13], and as coating and gluing  
40 sandwich panels for composite railway sleepers [14]. In these civil engineering applications,  
41 the epoxy-based polymer can be subjected to aggressive environmental conditions including  
42 in-service elevated temperatures, which can degrade this material. For example, Sirimanna et  
43 al. [15] measured a surface temperature as high as 61°C for FRP composite bridge decks  
44 exposed to Australian weather conditions. In such conditions, the main concern was the  
45 decrease of the mechanical properties due to material degradation from elevated  
46 temperatures.

47           The sensitivity of mechanical and physical properties of particulate-filled epoxy based  
48 resin to elevated temperatures is one of the major concerns in civil engineering and  
49 construction applications [16]. The continuous service temperature is generally known to be  
50 in the range of sub-ambient to 120°C [17]. Asset owners and engineers remain cautious about  
51 accepting epoxy matrices in civil infrastructure out of concern about their structural  
52 performance in the applications exposed to elevated temperatures. Manalo et al. [8]  
53 mentioned that the most important reason for this concern is the incomplete and limited  
54 information about the temperature dependence of composites for their application,  
55 particularly in hot areas. Polansky et al., [18] found that exposing epoxy-based FRP laminates  
56 to temperatures ranging from 170°C to 200°C and for a duration of 10 to 480 hours will  
57 rapidly decrease the material's glass transition temperature ( $T_g$ ) due the decrease in reaction  
58 to thermal stress. Their microscopic observations also showed degradation of epoxy resin  
59 (changing colour intensity) especially between the glass fibres and the matrix interface which  
60 led to gradual deterioration of electrical and mechanical properties. Anderson [19] further  
61 showed that the  $T_g$  of epoxy resin could remain constant for a short time, but rapidly  
62 decreased at elevated temperatures because they experienced network degradation as  
63 evidenced by mass loss. The mechanical properties of polymers are also noted to be  
64 significantly dependent on time and temperature [20, 21]. When exposed to high temperature,  
65 the epoxy polymer will soften and this can cause mechanical failures [22]. Ray [23] noted a  
66 high moisture absorption for glass and carbon fibre-reinforced epoxy composites with an  
67 increase in temperature. The high temperature during hygrothermal ageing also modified the  
68 local stress threshold required for delamination nucleation and reduced the interlaminar shear  
69 strength of epoxy-based composite laminates. Therefore, there is a need to explore methods  
70 to enhance the performance of epoxy resin under elevated temperatures.

71 Different additives were introduced to epoxies to improve their properties at an  
72 elevated temperature including nanocomposites with carbon-family materials and  
73 metal hydroxides. [24, 25]. Koh et al. [20] found that the fracture toughness and failure  
74 mechanisms of bisphenol A epoxy resin and cyclohexanedicarboxylic anhydride (hardener) at  
75 an elevated temperature can be enhanced by filling with silica particulates. Recent  
76 developments have also shown that the application of filler materials such as fly ash (FA),  
77 fire retardant (FR) fillers, hollow microsphere (HM), and silica can improve certain  
78 mechanical properties and at the same time, reduce the cost of epoxy-based polymer matrix  
79 and provide environmental benefits [26,27]. The mechanical behaviour of particulate filled  
80 epoxy resin is the result of complex interplay between the characteristics of the constituent  
81 phases: filler, resin, and interfacial regions [28]. The result of research by Bărbuță et al., [29],  
82 Rebeiz et al., [30], and Gorninski et al., [31] have shown that the inclusion of fillers could  
83 improve chemical, thermo-mechanical, mechanical, and durability properties of epoxy-based  
84 polymer concrete. Lokuge and Aravinthan [32] also noted an increase in compressive  
85 strengths as high as 100 MPa for epoxy-based polymer concrete with the addition of 10% FA  
86 by volume. Ferdous et al., [9] showed that the addition of light-weight fillers up to 60% by  
87 volume could increase flexural modulus around three times as the fillers provide a larger  
88 surface area that promotes rigid bonding with the resin. While these studies have shown that  
89 the addition of particulate fillers can improve mechanical properties of epoxy resin, very  
90 limited information exists on the effects of elevated temperatures to which civil  
91 infrastructures are normally subjected. A better understanding of the performance of  
92 particulate-filled epoxy based resin under an elevated in-service temperature must be  
93 achieved to further the safe use and adoption of this material in various construction  
94 applications.

95 In this study, experimental investigations were conducted to determine the effect of in-  
96 service temperatures on the durability of particulate-filled epoxy based resin containing FA  
97 and FR fillers. It focuses on understanding the effect of in-service elevated temperature on  
98 physical, mechanical, and physico-chemical properties as well as the microstructure of  
99 epoxy-based polymer matrix. The results of this research are expected to provide critical  
100 information to advance the application and development of durable cost-effective epoxy-  
101 based coating matrix through a comprehensive understanding and evaluation of their  
102 mechanical properties and degradation mechanism.

## 103 2. Materials and methods:

### 104 2.1. Materials

105 **Figure 1** shows the materials employed in this study including epoxy resin and lightweight  
106 fillers. The two main components of the epoxy resin system were Bisphenol A diglycidyl  
107 ether (DGEBA) type epoxy resin (Part-A) and an amine-based curing agent (Part-B). This  
108 type of epoxy system was previously studied by Ferdous et al. [4] and found suitable for  
109 composite railway sleeper application. The epoxy resin was supplied by ATL Composites Pty  
110 Ltd (Gold coast, Australia). Part A as unreactive and part B as reactive components were  
111 mixed together based on the Amine Hydrogen Equivalent Weight (AHEW) of 60 g for Part-B  
112 and Epoxy Equivalent Weight (EEW) of 190 g for Part-A as furnished by the supplier. One  
113 equivalent weight quantity of the amine curative and one equivalent weight quantity of  
114 DGEBA epoxy resin were required in order to make the resin mix reactive. Thus, 100 g of  
115 Part-A with density of  $1.064 \text{ g/cm}^3$  were used to mix with 32 g of Part-B with density of  
116  $1.182 \text{ g/cm}^3$  to maintain the mixing ratio. Two different fillers including FR (hydrated  
117 alumina powder) with a density of  $2.411 \text{ g/cm}^3$  and FA with a density of  $2.006 \text{ g/cm}^3$ , were  
118 mixed together. Railway sleepers are often subjected to fire from thermite welding of rail  
119 joints, elevated temperature and UV radiation from sun. This is why hydrated alumina  
120

121 powder and fly ash have been used together [33, 34]. The FR used was non-toxic and had low  
 122 abrasiveness, chemical inertness, acid resistance, smoke suppression and electric arc  
 123 resistance, and was supplied by Huber Engineered Materials (HEM), while Cement Australia  
 124 Pty Ltd supplied FA. The fillers were round with a diameter of 0.1 to 30  $\mu\text{m}$  for FA and 75 to  
 125 95  $\mu\text{m}$  for FR [14].



126  
 127 **Figure 1:** From left: Epoxy resin (Part-A), amine-based curing agent (Part-B), FR and FA

## 128 2.2.Mixture proportions

129 Four mixes with different amounts of filler were prepared, and the mix with no filler was  
 130 considered to be the control sample. Filler amounts of up to 60% by volume of the matrix  
 131 were added in increments of 20%, as more than 60% by volume filler in the mix was found  
 132 unworkable, as was also confirmed by Ferdous et al. [9]. The mixing ratio of FR-to-FA was  
 133 kept constant for all mixes. This ratio was adopted from the previous study [9] where it was  
 134 finalised after several trials. Since the main purpose of this study is to investigate the effect of  
 135 temperature on the mechanical and microstructure properties and ensure the cost is  
 136 minimised, therefore, the total amount of filler was considered as a variable rather than the  
 137 ratio of FR-to-FA. The mixes were denoted according to the amount of filler by volume, e.g.,  
 138 F20 indicates a mix containing 20% filler and 80% resin, as detailed in **Table 1**.

139 **Table 1:** Mix proportion of polymer matrices

Resin/Filler (by volume)	F0	F20	F40	F60
Part A (g)	1000	737	552	368

Part B (g)	320	236	177	118
FR (g)	0	397	794	1192
FA (g)	0	119	239	358

### 140 2.3.Specimen preparation

141 The preparation of samples and characterisation of the physical, mechanical, thermo-  
142 mechanical and microstructural properties of the epoxy polymer matrices were performed  
143 according to appropriate ASTM test standards. **Table 2** summarises the different test methods  
144 and the number of specimens tested for each type of test. The epoxy resin materials and the  
145 particulate filler materials were first mixed separately. This ensured consistent mixing and  
146 allowed the epoxy resin to become completely mixed and reactive before the filler was  
147 added, then they were all mixed together until the matrix had a uniform consistency. The  
148 specimens were cast in: i) sealed-bottom cylindrical PVC pipes with a diameter of 25 mm  
149 and height of 25 mm – suitable for measuring the density, porosity, compressive strength and  
150 split tensile strength; ii).non-stick sheets to be cut to 60 mm length, 10 mm width and 5 mm  
151 depth – suitable for measuring the  $T_g$ . The samples were cured in moulds for 2 days at room  
152 temperature, demoulded and then tested after 7 days.

153 **Table 2:** Summary of the test methods and number of specimens

Properties	Test Method	Number of specimens			
		F0	F20	F40	F60
<b>Physical properties</b>					
Density	ASTM C905 [35]	4	4	4	4
Porosity		5	5	5	5
<b>Thermo-mechanical properties</b>					
Dynamic Mechanical Analysis (DMA)	ASTM D7028 [36]	2	2	2	2
Simultaneous Thermal Analysis (TGA/DSC)		1	1	1	1
<b>Mechanical properties</b>					
Compressive strength	ASTM C579, [38]	15	15	15	15
Split tensile strength	ASTM C579 [38]	15	15	15	15
<b>Microstructure</b>					
Scanning Electron Microscopy		5	5	5	5



(SEM)

Micro-focused Fourier Transform  
Infrared Spectroscopy (FTIR)

5 5 5 5

---

154

### 155 3. Test procedure

#### 156 3.1. Physical Properties

##### 157 3.1.1. Density

158 The hardened density of different mixes with dimensions of 25 mm high and 25 mm in  
159 diameter was measured using an electronic balance (MonoBloc-AB204-S) with sensitivity of  
160 0.0001 g according to the ASTM C905 [35]. The weight and volume of demoulded samples  
161 were measured. The hardened density then was calculated according to the standard.

##### 162 3.1.2. Pore size

163 The size of the pores of different polymer matrices tested under various temperatures was  
164 measured using an optical microscope from the cut slices of 25 mm by 25 mm surface. A  
165 total of 60 images were taken, 3 from each sample exposed to various temperatures and with  
166 different percentages of fillers.

#### 167 3.2. Thermo-mechanical properties

##### 168 3.2.1. Glass transition temperature

169 To measure the  $T_g$  of different mixes, dynamic mechanical tests (DMA) were carried out  
170 according to the ASTM D7028 [36].  $T_g$  is one of the main thermal properties in polymeric  
171 composite materials.  $T_g$  is the temperature at which the state of polymeric material is changed  
172 from hard or glassy to rubbery and soft [18, 37]. A Q800 type TA instrument was used,  
173 wherein the samples were clamped by using a dual-cantilever system and the DMA multi-  
174 frequency strain of 1 Hz was applied. The temperature between 30°C and 120°C and  
175 increments of 5°C during temperature scans was set. At least two samples with dimensions of  
176 60 mm×10 mm×5 mm were tested for each series to determine the  $T_g$  of the epoxy-polymer

177 matrix. The surfaces of the samples were prepared straight, flat, clean and dry to prevent  
178 them slipping from the dual cantilever grips

### 179 3.2.2. *Loss of weight*

180 A calibrated simultaneous DSC/TGA (SDT 650) (Simultaneous Thermal Analysis)  
181 manufactured by TA Instruments was used for measuring the percentages of weight loss. Dry  
182 nitrogen gas at 200 ml/min was used during the experiments to purge the SDT cell. Samples  
183 between 10 and 25 mg were enclosed in the standard SDT aluminium sample pans. Dynamic  
184 scans were performed at a heating rate of 5°C/min from room temperature to 120°C. The  
185 moisture contents in the specimens were determined by SDT analysis as the difference in the  
186 weight loss between the reference matrix and the material under investigation and dried up to  
187 120°C.

### 188 3.3. Mechanical Properties

189 The compressive and splitting tensile strength of polymer filled epoxy matrix were evaluated  
190 at five different temperatures (23, 40, 50, 60 and 80°C) to coincide with in-service  
191 temperatures for epoxy thermosets as suggested by [16]. In order to achieve the required test  
192 temperature, Instron 3119 environmental chamber mounted on a 100kN servo-hydraulic MTS  
193 machine was used. Before testing, a smooth surface had been prepared for the cylindrical  
194 samples to facilitate the uniform distribution of load. The environmental chamber was firstly  
195 set for 30 min at the required temperature before testing. Meanwhile, the other samples were  
196 placed in an oven set at the desired temperature while the testing of samples at a lower test  
197 temperature was being conducted. This was in addition to the 30 min soaking period in the  
198 chamber. The splitting tensile and compressive strength of the samples were obtained in  
199 accordance with the test procedure in the ASTM C579 [38] using 100 kN universal testing  
200 machine with a loading rate of 2 mm/min.

### 201 **3.4.1 Scanning electron microscope**

202 The scanning electron microscope (SEM) observation was carried out to investigate the  
203 microstructural characteristics of the different polymer mixes tested under different  
204 temperatures by using (SEM, JEOL JXA 840A). The samples were carefully prepared by  
205 cutting into small pieces (dimensions <1 cm) and then coated by gold using a sputter  
206 deposition machine. Afterward, the SEM was performed on the various small gold-coated  
207 pieces.

### 208 **3.4.2 Fourier-Transform Infrared spectroscopy**

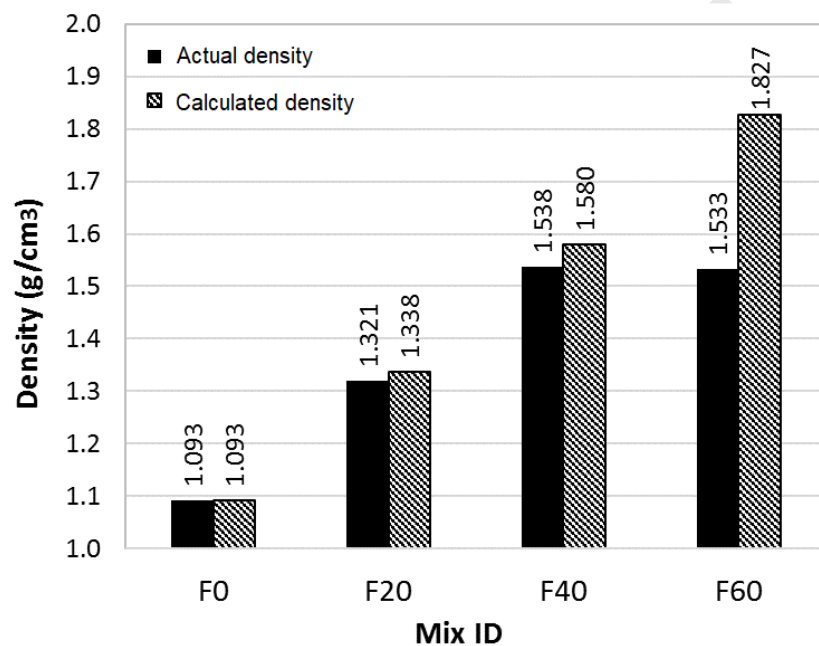
209 Microfocused Fourier-transform infrared spectroscopy (FTIR) was conducted in order to  
210 determine the functional groups presented in the particulate filled epoxy base resin. FTIR  
211 spectra were recorded on a Nicolet 6700 FTIR spectrophotometer with KBr pellets. Spectra  
212 in the optical range of 400–4000 $\text{cm}^{-1}$  were then achieved by averaging 16 scans at a  
213 resolution of 4  $\text{cm}^{-1}$ .

## 214 **4 Results and Discussion**

### 215 **4.1. Effect of percentage of fillers and temperature on physical properties**

216 **Figure 2** shows the hardened densities of all epoxy mixes. It can be seen that the density  
217 increased (from 1.093  $\text{g/cm}^3$  to 1.538  $\text{g/cm}^3$ ) with an increase in filler content. This increase  
218 was up to approximately 40% in F40 compared to F0. The increase in density of the  
219 particulate filled resin can be explained by the replacement of lighter epoxy resin with fillers.  
220 This is to be expected as the density of filler (FR with a density of 2.411  $\text{g/cm}^3$  and FA with a  
221 density of 2.006  $\text{g/cm}^3$ ) was higher than that of the resin system (1.193  $\text{g/cm}^3$ ). However, the  
222 mix with 60% filler resulted in a slight reduction in the density of mixes compared to that of  
223 the F40 because the decrease in flowability of the mix resulted in the creation of more pores  
224 and voids than the mixes with a lower amount of fillers. The densities of the polymer-filled  
225 epoxy based matrix with different components were also calculated (**Figure 2**). From the

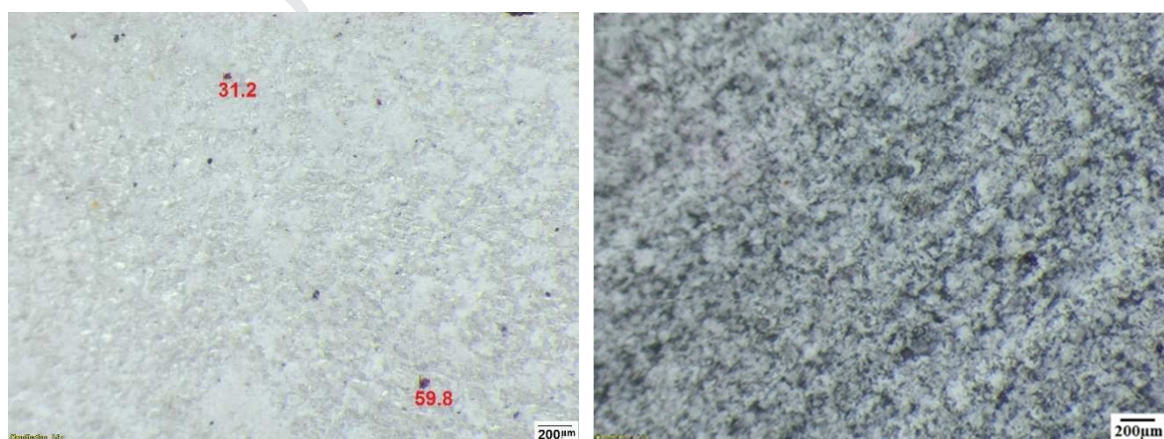
226 combined densities of the components in the mix, it was found that the densities of the mixes  
 227 increased from 1.093 g/cm<sup>3</sup> to 1.827 g/cm<sup>3</sup> with increase in the filler volume from 0% to  
 228 60%. Based on the experimental results, it was observed that the variation between the  
 229 calculated and the measured densities increased with the increase in the amount of fillers.  
 230 This variation was almost 16% for F60. This further shows that the mix containing 20% filler  
 231 volumes was flowable, which was due to low viscosity of epoxy resin. However, the  
 232 inclusion of 40% or more fillers produced filler-dominated matrices.



233  
 234 **Figure 2:** Density of different epoxy mixes

235 The variations in density of the particulate-filled resin can be explained by the measured  
 236 porosity of the mix. **Figure 3** shows that the pore sizes and number of the samples increased  
 237 with increments of filler percentages from 0% to 60%. These pores were small for the mixes  
 238 with 20% filler but relatively big for 60% filler. These findings were in agreement with the  
 239 variations in density in **Figure 2**, where differences between the densities of the solid and  
 240 ingredients samples were higher in mixes including higher volume of fillers. Based on the  
 241 results of Ferdous et al., [9], the inclusion of particulate fillers not only led to an increase in  
 242 density to the peak of 1.458 g/cm<sup>3</sup> in F60, which is close to that of the timber railway

243 sleepers, but also increased the porosity from 0.02% in F0 to 4.37% in F60. This showed the  
244 effect of fillers in the pore structure of epoxy based polymer matrix. **Figure 4** also shows the  
245 porosity of the surfaces of samples without fillers tested at 60°C and 80°C. Compared to  
246 **Figure 3a** which showed the porosity of the F0 at room temperature, it is obvious from  
247 **Figure 4a** that by increasing the temperature to 60°C, the volume and size of the pores  
248 reduced. The size of the pores of F0 further reduced at 80°C as shown in **Figure 4b** (from 60  
249  $\mu\text{m}$  at room temperature to 18 $\mu\text{m}$  at 80 °C). The trend was similar for F60 as can be seen in  
250 **Figure 5**, wherein the increase of temperature showed a significant decrease on the volume  
251 and size of the pores compared to that at room temperature (**Figure 3d**) (from 402 $\mu\text{m}$  at room  
252 temperature to 73 $\mu\text{m}$  at 80°C). This can be due to softening and increasing of the mobility of  
253 the epoxy resin molecules at higher temperatures and decreasing the pore size in the samples  
254 including fillers. It has been reported that an increase in temperature can lead to a decrease of  
255 pores in the mix [39]. Lin and Ritter [40] also conducted a study on the effect of temperature  
256 on the pore structure of carbon xerogels derived from resorcinol–formaldehyde resins. They  
257 found that increasing the carbonisation temperature caused a reduction in the number of  
258 micropores, and it also had effect on the mesopore size distribution.



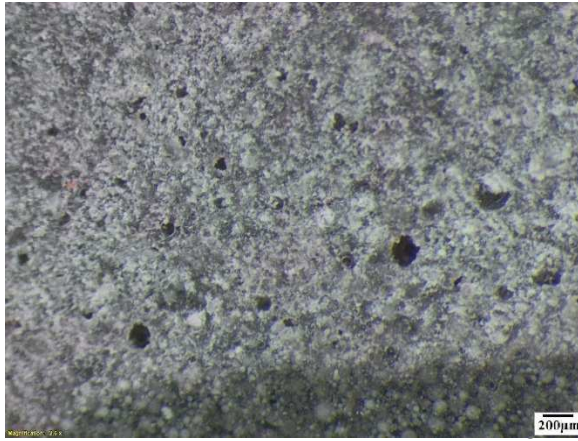
259

(a) F0

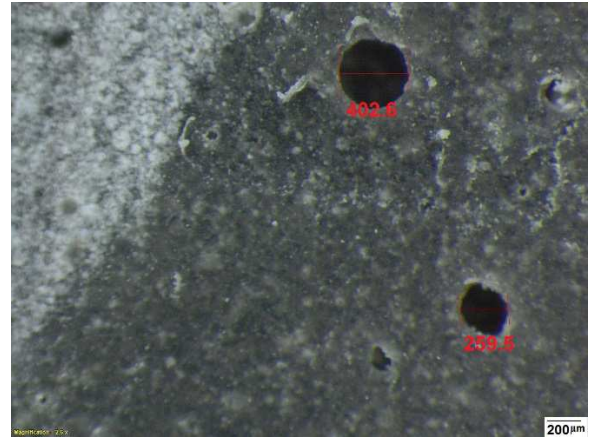
(b) F20

260





(c) F40

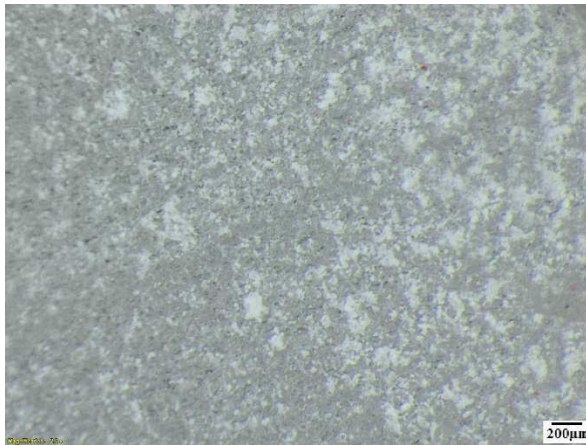


(d) F60

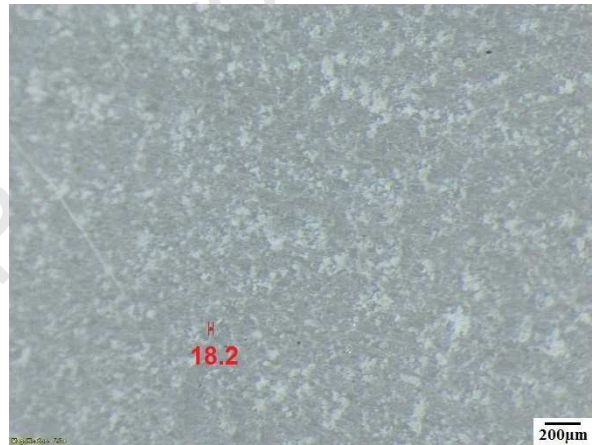
262

263

**Figure 3:** Porosity of epoxy based resin with different amount of fillers



(a) 60°C



(b) 80°C

264

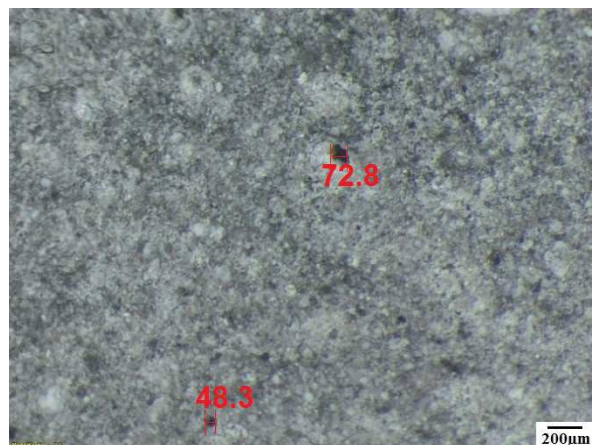
265

266

**Figure 4:** Porosity of F0 at elevated temperature



(a) 60°C



(b) 80°C

267

268

269

**Figure 5:** Porosity of F60 at elevated temperature

## 270 4.2. Effect of percentage of fillers and temperature on thermo-mechanical properties

271 The effect of percentage of fillers and temperature on thermo-mechanical properties of the  
272 particulate filled epoxy resins was evaluated using the Dynamic Mechanical Analysis  
273 (DMA). In addition, the Simultaneous Thermal Analysis (SDT) was conducted to measure  
274 weight loss at elevated temperatures to characterise the thermal stability of the particulate  
275 filled epoxy resin. The DMA results in **Figure 6a** revealed three different temperature zones  
276 that affect the storage modulus of the polymer matrices: i) a reference plateau between 30°C  
277 and 55°C, where stiffness remained almost stable; ii) a zone that caused considerable  
278 decreases in between 55°C and 65°C, where temperatures were near  $T_g$ ; and iii) a zone that  
279 caused slight decreases in storage modulus between 85 and 120°C, where the temperature  
280 was above the  $T_g$  of the polymers. In zone (i), since the temperature was below  $T_g$ , the  
281 molecular chain mobility of the polymer did not change, as also indicted by Ashrafi et al.,  
282 [41]. By increasing the temperature to 55°C and reaching the  $T_g$  in zone (ii), the molecular  
283 bonds began breaking and caused the ductility of the material to increase, resulting in a  
284 significant reduction in the storage modulus of the samples. In the last zone (iii), there was a  
285 gradual decrease in the storage modulus.

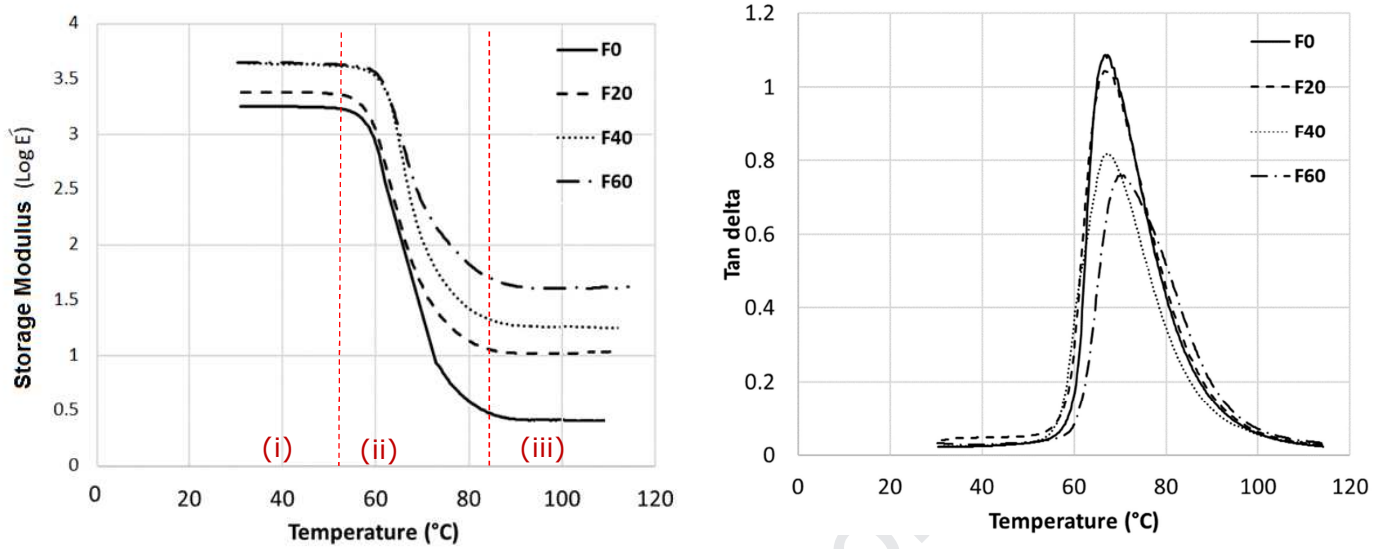
286 From the storage modulus curve in **Figure 6a**, it can be seen that the  $T_g$  of F0 is at 57°C  
287 while that of F60 is at 63°C. On the other hand, the measured  $T_g$  from the tan delta curve in  
288 **Figure 6b** for F0 is 65°C while that of F60 is 70°C. This result indicated that adding up to  
289 60% of filler to the polymer matrix increased the  $T_g$  by 5-6°C. This enhancement in the  
290 thermo-mechanical properties of epoxy resin is directly related to the higher capability of a  
291 polymer matrix with fillers to store energy under high temperatures due to high thermal  
292 resistance of the used fillers [9]. The  $T_g$  of the polymer mixes depended basically on the resin  
293 system, while the type of resin was the same for different mixes. However, when the fillers  
294 with higher degradation points (Epoxy resin-340°C, FA-800°C and FR-980°C) were included

295 in the matrix, it led to an increase in the  $T_g$  as well. Shamsuddoha et al. [42] also showed that  
296 the incorporation of coarse aggregates could increase the storage modulus and  $T_g$ . In their  
297 research it was found that the  $T_g$  for the mix containing 45% epoxy resin and 32% fine filler  
298 (0.06 – 350.0  $\mu\text{m}$ ) with 23% hardener, was around 38°C, while with the incorporation of 60%  
299 coarse aggregates (40.45  $\mu\text{m}$  – 2.36 mm), it was boosted to 60°C. Ferdous et al. [9] also  
300 revealed that the  $T_g$  was increased with the increase of FA, FR and HM percentages, where in  
301 different mixes, the magnitude of  $T_g$  ranged from 50°C to 55°C using the storage modulus.  
302 Moreover, **Figure 6b** shows that the magnitude of the peak of the tan delta as a function of  
303 temperature decreased from 1.05 to 0.76 with the increases in the filler percentage to 60%.  
304 These results indicated that F0 with tan delta peak of 1.05 has more potential for energy  
305 dissipation than the mixes with higher amount of filler as tan delta represents the ratio of the  
306 dissipated energy (loss modulus) to the energy stored (storage modulus) per cycle sample  
307 deformation. Energy dissipation is the result of an irreversible process in which energy is  
308 transformed from initial form to final form, while the capability of the final form in term of  
309 mechanical resistance is less than the initial form. Crosslink is a covalent bond formed when  
310 epoxy molecules react with curing agent molecules. In crosslinking reactions of DGEBA and  
311 hardener, the C-O bond within the epoxide group breaks and the carbon end of the opened  
312 epoxy group reacts with the nitrogen of the amine group in the curing agent molecule [43].  
313 Crosslink density ( $\nu_c$ ) is directly related to the storage modulus ( $E'$ ) in the rubbery plateau  
314 region according to the following equation [44]:

$$315 \quad E' = \nu_c RT \quad (2)$$

316 where T is the temperature (K) and R is the gas constant. As shown in **Figure 7**, the  
317 crosslinking density increased with further inclusion of fillers. F60, which has the highest  
318 amount of fillers, has the highest storage modulus and consequently crosslink density is  
319 increased.





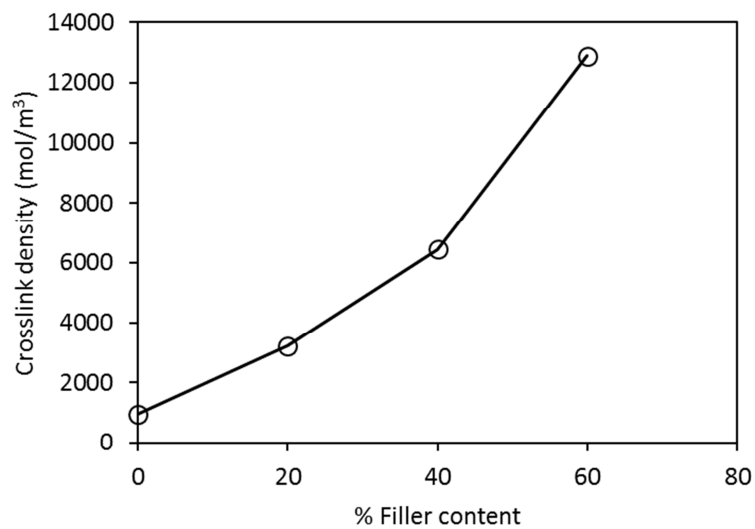
320

321

(a) Storage Modulus

(b) Tan delta

322

**Figure 6.** Variations in dynamic mechanical properties with temperature

323

324

**Figure 7.** Crosslinking density of particulate filled epoxy polymer

325

326

327

328

The temperature at which the rapid loss of weight occurs can be also defined as the decomposition temperature. It is the temperature, under which the thermoset loses its weight most rapidly during the whole degradation process [45]. In many applications, adhesive strength loss is a significant variable, which leads to ambiguity in how loss of weight

329 measurements is related to loss of adhesive strength at the anticipated in-service temperature.  
330 **Table 3** shows the weight loss of different mixes which was evaluated by SDT from the room  
331 temperature to 120°C, similar to the temperature range for the DMA test. Neat epoxy resin  
332 exhibited a minor loss of weight of around 0.02% at lower temperature and then a rapid  
333 weight loss of around 0.63% at 120°C, possibly due to loss of water or unreacted volatiles,  
334 which come from amine-based organic compound of hardener as indicated by Preghenella et  
335 al. [46]. As a measure of the extent of degradation, the extent of weight loss is usually applied  
336 . Volatile degradation species that are released from the material when network bonds break,  
337 can lead to weight loss. It is worth noting that the extent of degradation definition is not  
338 implying 100% loss of weight at an extent of degradation of unity. The ultimate weight of the  
339 sample, which is asymptotically approached over a long time is referenced by the extent of  
340 reaction [17]. Thus, this significant weight loss for F0 is predicted to be followed at higher  
341 temperatures due to the thermal degradation of the resin matrix, which will result in a  
342 considerable weight loss of the epoxy resin. However, F40 and F60 showed significantly less  
343 weight loss of only around 0.2% and 0.07%, respectively at 120°C. This phenomenon can  
344 play an important role in improving the retardant properties of the epoxy polymer due to their  
345 higher ability to store the energy under high temperatures as was already indicated in **Figure**  
346 **6a**.

347 The result of weight loss is in agreement with the measured  $T_g$  result.  $T_g$  and weight  
348 loss are two important properties showing the influence of degradation, and demonstrate that  
349 the inclusion of fillers can help to reduce the degradation rate under elevated temperatures.  
350 Thus, the thermal stability of the epoxy at high temperatures was improved, as the  
351 percentages of resin was reduced by inclusion of FA and FRA in the mixes due to the higher  
352 melting temperature of the particulate fillers compared to that of the epoxy resin.

353 **Table 3:** Weight losses after SDT scan

Mix ID	(40°C) %	(60°C) %	(80°C) %	(100°C) %	(120°C) %
F0	0.0202	0.0814	0.1789	0.4230	0.6238
F20	0.0240	0.0755	0.1573	0.2894	0.4486
F40	0.0183	0.0689	0.1122	0.1611	0.2045
F60	0.0009	0.0093	0.0331	0.0656	0.0765

354

355 **4.3 Effect of percentage fillers and temperature on mechanical properties**

356 The mechanical properties of the epoxy-based polymer with different percentages of fillers  
357 and at elevated temperature were assessed under compression and split tensile testing. **Table**  
358 **4** summarises the results of the mechanical tests. In order to have a fair comparison of strength  
359 among the mixes with different densities, the specific strength also has been provided. The values  
360 listed within parentheses are the standard deviation of the test results.

361 **Table 4:** Mechanical properties of epoxy polymer matrices under elevated temperature

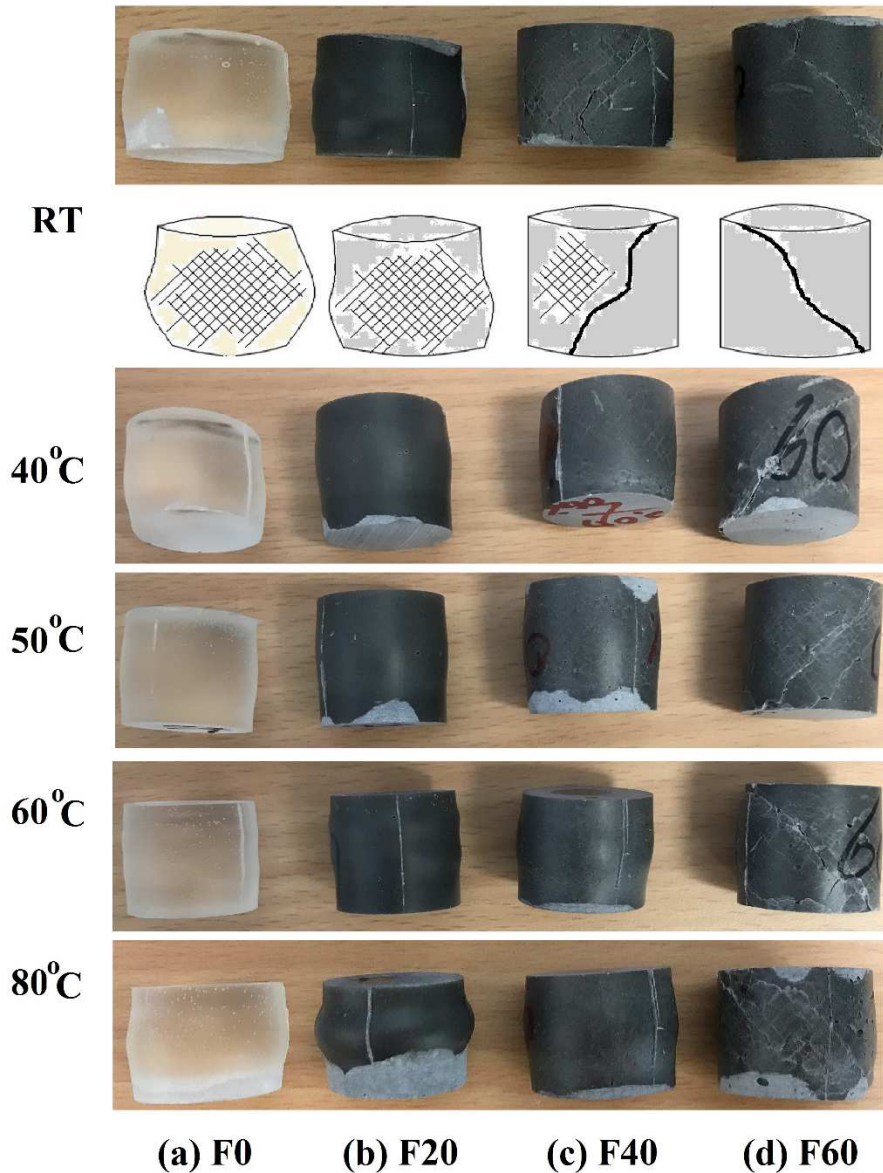
Property		Temperature									
		Room		40°C		50°C		60°C		80°C	
Mix ID	Density	strength	Specific strength	strength	Specific strength	strength	Specific strength	strength	Specific strength	strength	Specific strength
Compressive strength (MPa)											
F0	1.093	92.0 (3.3)	84.2	51.2 (1.4)	46.8	25.2 (2.5)	23.1	3.1 (0.6)	2.8	1.4 (0.7)	1.3
F20	1.321	85.7 (2.9)	64.8	52.8 (1.8)	39.9	33.4 (2.2)	25.3	7.3 (1.6)	5.5	5.3 (0.6)	4.0
F40	1.538	82.4 (2.3)	53.6	58.7 (0.1)	38.2	45.1 (3.8)	29.3	37.0 (2.1)	24.1	34.4 (0.0)	22.3
F60	1.533	59.4 (6.7)	38.7	47.4 (0.2)	30.9	44.3 (6.4)	29.0	43.5 (1.7)	28.4	43.1 (3.7)	28.1
Splitting tensile strength (MPa)											
F0	1.093	33.9 (1.4)	31.0	15.8 (1.3)	14.4	3.8 (1.6)	3.5	1.0 (0.7)	0.9	0.7 (0.2)	0.6
F20	1.321	27.1 (0.8)	20.5	19.3 (1.2)	14.6	10.3 (3.8)	7.8	3.7 (3.4)	2.8	3.2 (1.9)	2.4
F40	1.538	25.3 (1.7)	16.5	17.9 (1.3)	11.6	14.8 (3.2)	9.6	10.3 (5.4)	6.7	9.5 (1.5)	6.1
F60	1.533	20.4 (0.7)	13.3	15.7 (0.7)	10.2	12.3 (1.0)	8.0	12.1 (2.1)	7.9	10.8 (0.7)	7.0

362

363 **Figure 8** shows the typical failure mode of particulate-filled epoxy resin in compression at  
364 elevated temperature. As shown in **Figure 8**, despite the creation of micro cracks, which were  
365 not easy to see with the naked eye, specimens F0 and F20 were deformed without crushing  
366 even after reaching their ultimate strengths (**Figure 8 a and b**). These samples behaved like

367 elastic materials as they resumed their original shape when the load was released, even  
368 though they retained some of their bulged shape. On the other hand, at lower temperatures,  
369 micro cracks followed by a shear cracks were observed for specimen F40. It is interesting to  
370 note that for F60, noticeable failures with a huge sudden shear crack at ultimate strength was  
371 observed, showing a brittle fracture. The stiffness of fillers can be attributed to the  
372 mechanisms of this phenomenon for those mixes containing higher percentages of filler,  
373 particularly F60 as was also reported by Ferdous et al., [9]. Indeed, the behaviour of polymer  
374 matrices changed from flexible to relatively rigid with an increase in the volume of filler,  
375 which is also indicated by the abrupt drop in the stress strain curve in the next paragraph. The  
376 failure mode could be also related to pore size and volume. The increase of porosity with the  
377 increase of fillers also affected the transfer of stresses from one part to another that may  
378 increase stress concentration and lead to premature failure. High-porosity mixes (F40 and  
379 F60) have larger pores randomly distributed through a matrix and failed in a brittle manner.  
380 However, the crack along the direction of the compressive stress rather than along the  
381 interface between the resin and the fillers, indicates the excellent adhesion of fillers to the  
382 epoxy matrix. Similarly, Ferdous et al. [9] found that epoxy-based polymer containing up to  
383 30% of FA, FR and HM exhibited an elastic failure mode without visible cracks under  
384 compression at room temperature while the samples including 40%, 50% and 60% failed by  
385 cracking. One can observe that the failure modes for resin-rich mixes at higher temperatures  
386 are similar to those at room temperature, indicating flexible matrices. However, it was also  
387 apparent that the failure mode in F40 became flexible under elevated temperature and it was  
388 followed by microcracks and bulged shape. For F60, a semi-ductile failure can be observed at  
389 higher temperatures; the failure was initiated as a microcrack, then propagated as a shear  
390 failure that resulted in multiple fracture and crushing under ultimate load. With an increase in  
391 the temperature, as  $T_g$  was reached, the epoxy resin became very ductile. Meanwhile, the

392 inclusion of fillers could hinder the mobility of the polymer's molecular chains, and provide  
 393 some stiffness too. The strength retention at this temperature, which will be discussed in the  
 394 last paragraph, proves that the softening of the matrix allowed the fillers to move freely in the  
 395 direction of the loading, and their porosity decreased, resulting in a better stress transfer [39].  
 396 The reduction in porosity might consequently result in a decrease of brittleness.



397

398 **Figure 8:** Failure modes of particulate-filled resin under compression at different

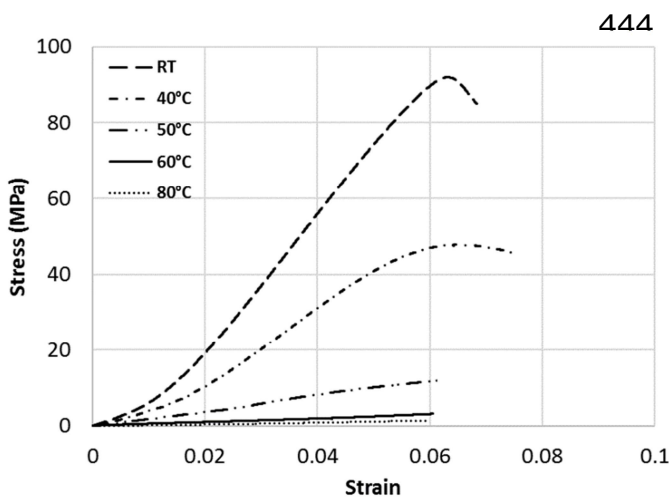
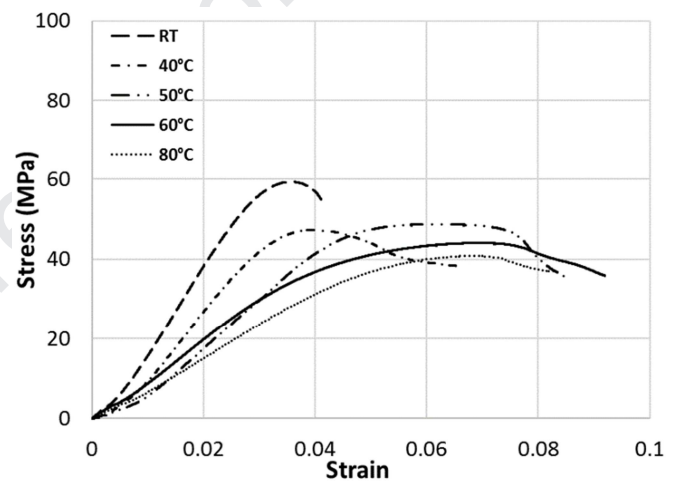
399

temperatures

400 The compressive stress and strain behaviour of F0 as reference and F60 as the mix containing  
401 the highest percentage of filler at room temperature to 80°C are plotted in **Figure 9**. For F0,  
402 slightly non-linear stress-strain behaviour is observed due to its nature of rubber-like  
403 material. The non-linearity then gradually reduced with an increment of filler content and  
404 became almost linear for the mix containing 60% fillers (**Figure 9b**). It is noticeable that at  
405 room temperature F60 has a lower failure strain compared to F0. This is caused by the  
406 introduction of particulate fillers in the epoxy with larger surface area and the creation of a  
407 rigid bond with the resin [9]. This consequently demonstrated an inflexible polymer matrix  
408 due to gradual increases in the volume of higher-modulus materials exhibiting a lower failure  
409 strain (**Figure 9b**) as it is also comparable in **Table 4**. However, with the increase of  
410 temperature in addition to retaining the properties, F60 exhibits a significant decrease in  
411 stiffness with an increase in failure strain. At high temperature, it showed more ductility due  
412 to the softening of the epoxy resin which led to an increase in bonding to fillers resulting in  
413 retaining strength at higher temperatures.

414 **Figure 10** shows the strength retention in compression of particulate filled epoxy-  
415 based resin at elevated temperature. In general, the compressive strength of epoxy-based  
416 polymers decreased with increasing temperature. This reduction in strength was caused by  
417 the softening of the epoxy matrix with the increase in temperature. Generally, higher strength  
418 retention was observed for the mixes containing filler compared to the neat epoxy due to the  
419 better filler and matrix interaction, which could be due to the reorientation of the fillers  
420 during the softening of the resin. Moreover, the softening of the resin and reduction in  
421 porosity resulted in the bonding between the filler and the resin being slightly enhanced. This  
422 result was supported by higher  $T_g$  and cross linking density of mixes with higher amount of  
423 fillers. As shown in **Figure 10** for samples without or with low amount of fillers (F0 and  
424 F20), there was a significant drop in the strength retention capacity at 60°C due to exceeding

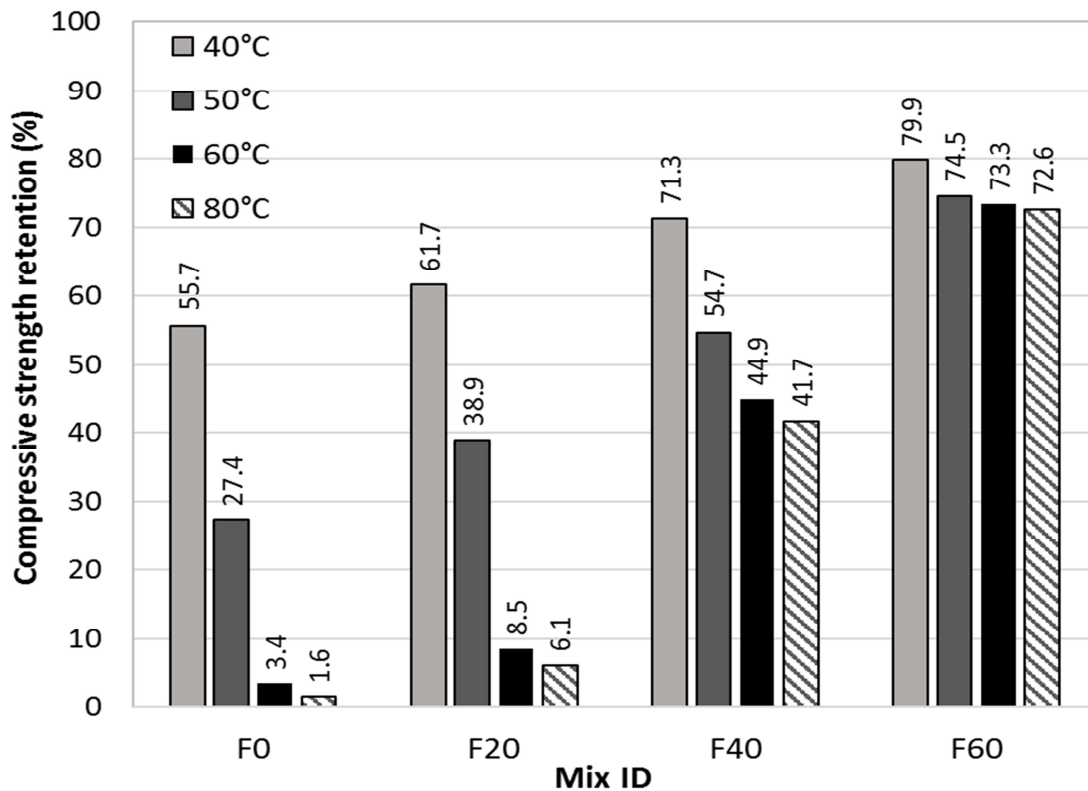
425 the  $T_g$  of polymer. When the temperature increased to 60°C (about their  $T_g$ ), epoxy reached  
 426 the heat distortion temperature (HDT), and it began to deform. The continued increase in  
 427 temperatures to 80°C led to more ductile and elastic behaviour and yield point and strength  
 428 loss. At this level of temperature, F0 and F20 retained only 3.4% and 8.5% respectively of  
 429 their compressive strength at room temperature. The low compressive strength retention of  
 430 mixes with low amount of particulate fillers can be directly linked to the softening of epoxy  
 431 resin at a temperature near or above  $T_g$  and losing its adhesive and cohesive strength, as was  
 432 also found by Bajracharya et al. [47]. On the  
 433 other hand, F40 and F60 could retain 44.9% and  
 434 73.3% respectively of their compressive strength  
 435 at 60°C, and 41.7% and 72.6% respectively at  
 436 80°C. The higher compressive strength retention  
 437 for F40 and F60 was firstly due to the better  
 438 thermal properties of the fillers including higher  
 439  $T_g$  and higher thermal stability as was discussed  
 440 in previous sections. Thus, the polymer filled epoxy can continue to support a load in higher  
 441 temperatures. This could be due to the softening of epoxy resin at higher temperatures, which  
 442 led to a reduction in the size and amount of pores in the mixes with higher percentages of  
 443 fillers as is shown in **Figure 8**.



(a) F

**Figure 9:** Compressive stress and strain behaviour at in-service elevated temperature





449

450

**Figure 10:** Compressive strength retention at in-service elevated temperature

451

452

453

454

455

456

457

458

459

460

461

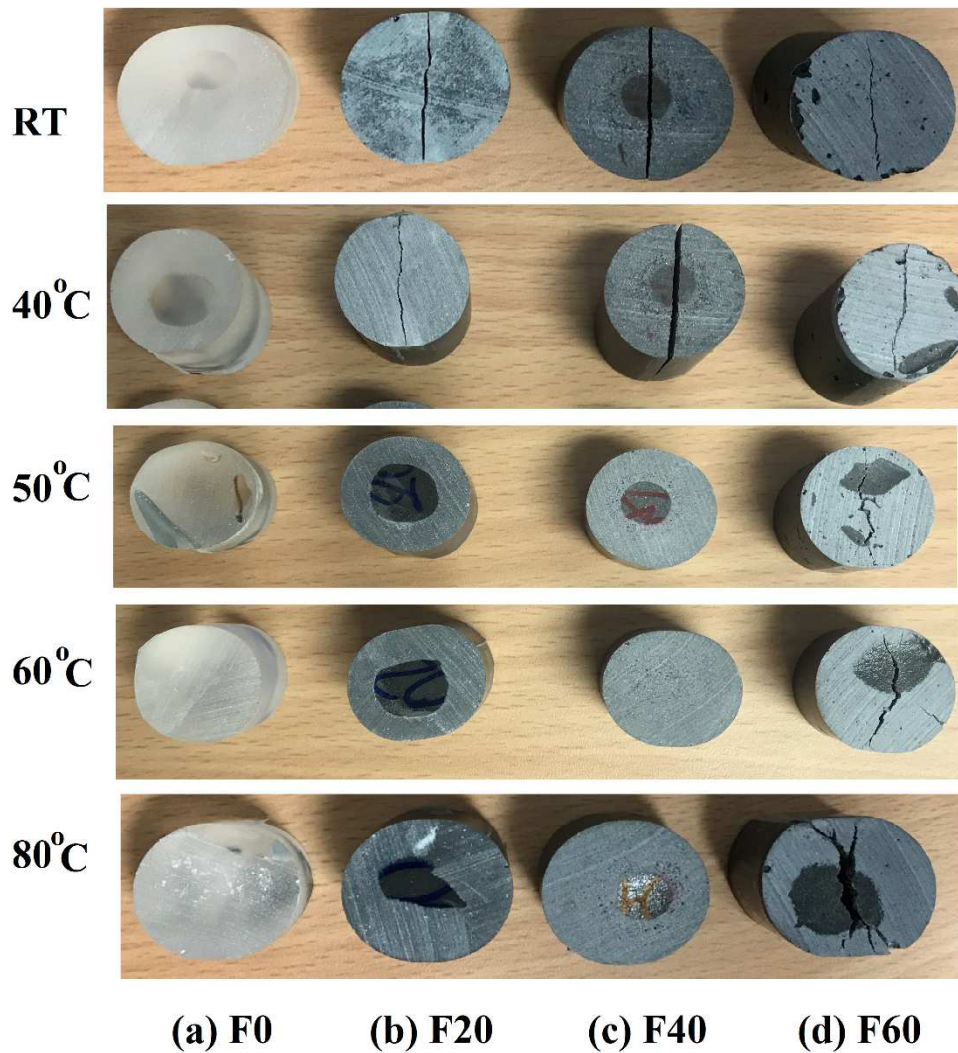
462

463

**Figure 11** shows the failure mode of various mixes after a splitting tensile test at room temperature and at the maximum temperature of 80 °C. As can be seen in **Figure 11**, in the same way as the samples tested under compression strength, F0 samples behave like elastic material and they deformed without visible cracks even after reaching their ultimate strengths; the samples resumed their original shape when the load was released. However, mixes containing 20%, 40% and 60% fillers failed primarily at a single cross section along the diameter by brittle fracture, which was followed by the abrupt drop in the stress-strain curve at peak load. This was due to the poor filler/matrix adhesion. At 80 °C, although F0 showed the same failure mode as room temperature, F20 and F40 showed ductile failure, which is due to the softening of epoxy resin at higher temperatures. The softening of the matrix allowed fillers to have better bonding with epoxy resin through the matrix, resulting in the increase in failure strength and flexibility of the matrix. F60, however, showed a semi-brittle fracture with inclined failure surface along the width of the sample tested at maximum



464 temperature of 80 °C. The resin transfers stress however, as the temperature increased, caused  
 465 the resin to become malleable and soft, thus, better interlocking between resin and fillers was  
 466 achieved.

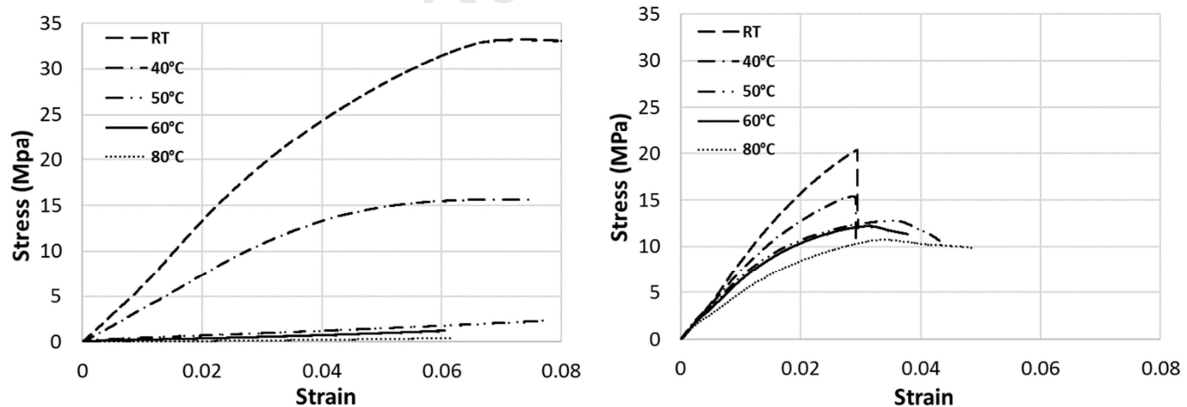


467

468 **Figure 11:** Failure modes of particulate-filled resin under tension at different temperatures

469 From **Figure 12**, stress-strain graphs show that at lower temperatures, F60 was completely  
 470 brittle, while F0 was ductile. Moreover, split tensile results at **Table 4** show the reduction of  
 471 strength with increasing filler volumes at room temperature due to gradual increases in the  
 472 amount of higher stiffness filler materials. This result is in agreement with the trend reported  
 473 by Lokuge and Aravinthan [32], who revealed that when the epoxy content was further

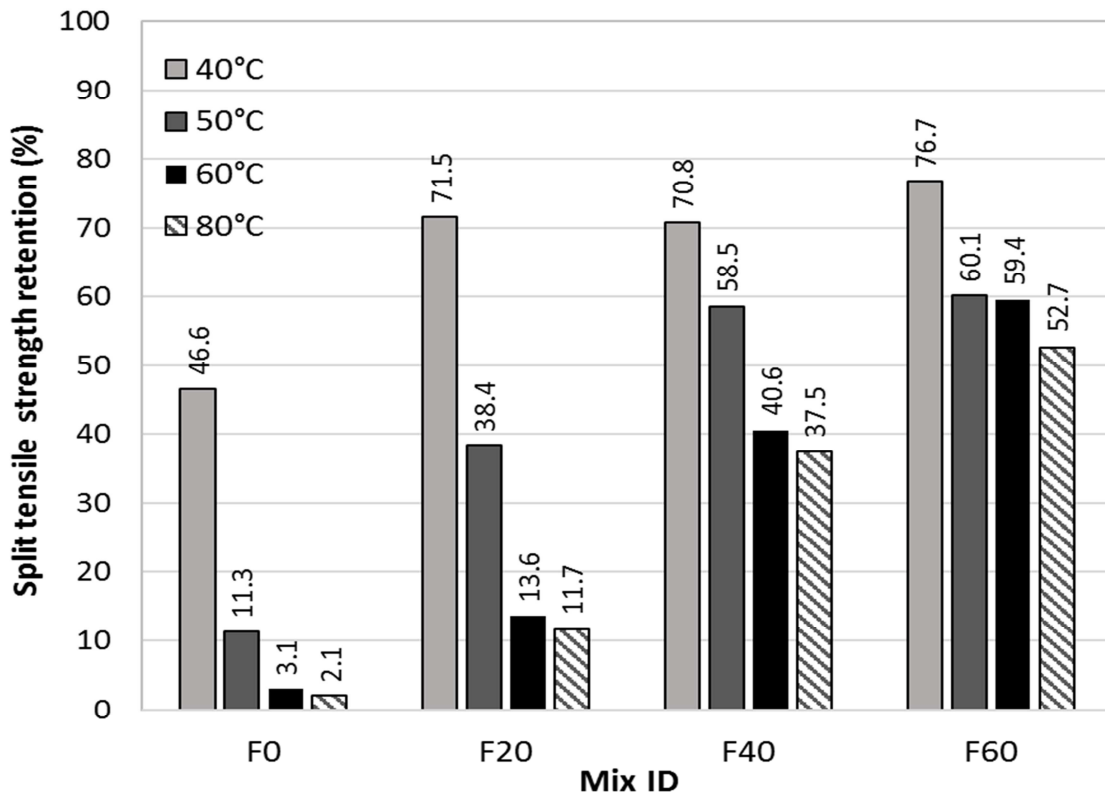
474 increased (20%), in addition to flexural strength and compressive strength, split tensile  
 475 strength also reduced. However, as the temperature reached 80°C, not only could F60 retain  
 476 more than 50% of the peak stress but also the tensile failure strain of F60 increased by the  
 477 rise in temperature. This phenomenon happened while neat epoxy resin was deformed under  
 478 minimal stress of less than 2-3 MPa at maximum temperatures of 60 °C and 80 °C. The  
 479 significant variations in strength for F0 and F20, which was observed with an increase in the  
 480 temperature was due to the softening of epoxy resin and a loss of the properties in resin-rich  
 481 mixes. The split tensile retention results given in **Figure 13** revealed that the inclusion of  
 482 higher percentages of fillers to the matrix could significantly help to retain the strength by  
 483 almost 41% and 37% for F40, and 59% and 53% respectively for F60 at 60°C and 80°C.,  
 484 Resin-rich samples (F0 and F20) significantly lost their strength particularly after 60°C. F0  
 485 experienced a significant reduction of 97% and 98% respectively in its strength at 60 °C and  
 486 80°C.,



(a) F0

(b) F60

489 **Figure 12:** Tensile stress and strain behaviour at in-service elevated temperature



490

491

**Figure 13:** Tensile strength retention at in-service elevated temperature

492

#### 4.5 Microstructure of particulate-filled epoxy resin at elevated temperature

493

494

495

496

497

498

499

500

501

502

503

504

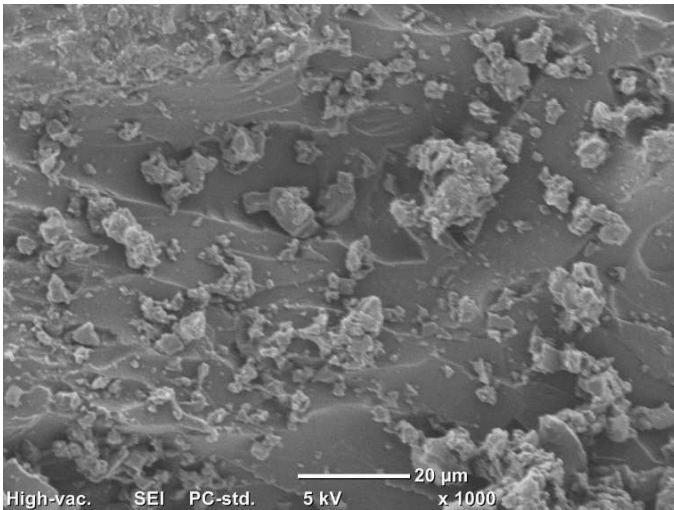
When materials are combined, their properties are governed not only by the characteristics of individual components, but also by the interface between them [48]. Moreover, the mechanical characteristics of a particulate filled polymer depend on the type of distribution of particles, which can be characterized by SEM [49]. From this study, the SEM revealed that the microstructure of F0 and F60 specimens has a direct correlation on the physical, thermo-mechanical and mechanical properties of epoxy-based polymer exposed to in-service elevated temperatures (**Figure 14**). Specimen F60 was chosen since it exhibited the highest property retention at 80°C. The FTIR of specimen F0 was also analyzed and presented for comparison. As can be seen in **Figures 14a and 14c**, there are remarkable differences in the texture and form of the particulate-filled epoxy resin compared to the neat epoxy samples. Dense microstructures with small pore sizes were formed in samples without filler (F0), while the mix containing 60% FA and FR (F60) showed various pores and weak

505 interfacial bond between different fillers and the resin through the matrix due to pores and  
506 voids in the matrix (**Figure 14c**). This subsequently decreased the mechanical performance of  
507 the polymer matrix at room temperature. Ahmad et al. [50] pointed out that the presence of  
508 fused silica resulted in inhomogeneous distribution and weakened the interaction between the  
509 matrix and the filler due to the defect in the matrix caused by the voids between the particles,  
510 and led to undesirable material properties.

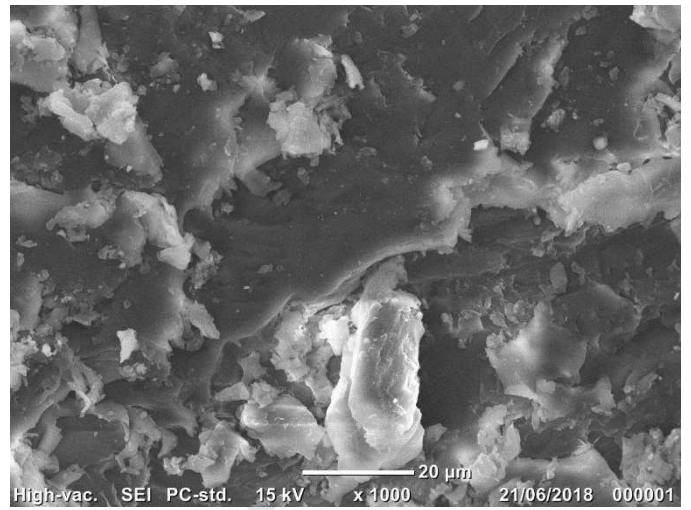
511 As shown in **Figure 14a**, F0 samples at room temperature have a compact but  
512 relatively rough surface even after the application of the load while after testing at 80°C, the  
513 roughness of fracture surface of epoxy samples was reduced (**Figure 14c**). On the other  
514 hand, a close inspection of **Figure 14c and 14d** revealed that the exposure of F60 to 80°C not  
515 only reduced the amount of pores but also improved the interfacial bond between the fillers  
516 and resin compared to room temperature (**Figure 14c**). For FR and FA as spherical  
517 inclusions, the packing arrangement defines the quantity of fillers and the distribution of  
518 particles. Thus, when the temperature increased, it enabled a better distribution of particles  
519 and consequently a dense microstructures with lower pores or voids formation. This then  
520 helped to retain the mechanical strength and increase the strain failure. This was in agreement  
521 with the results reported in the physical section, wherein the increase of temperature led to a  
522 significant decrease on the number and size of the pores (**Figures 3b and 5b**).

523





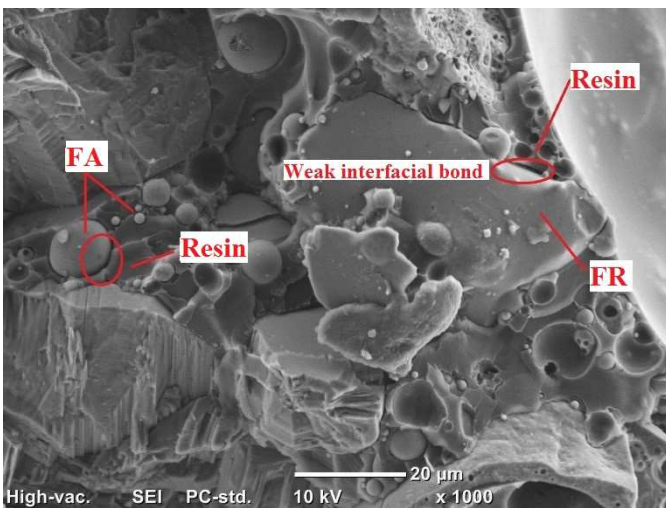
524



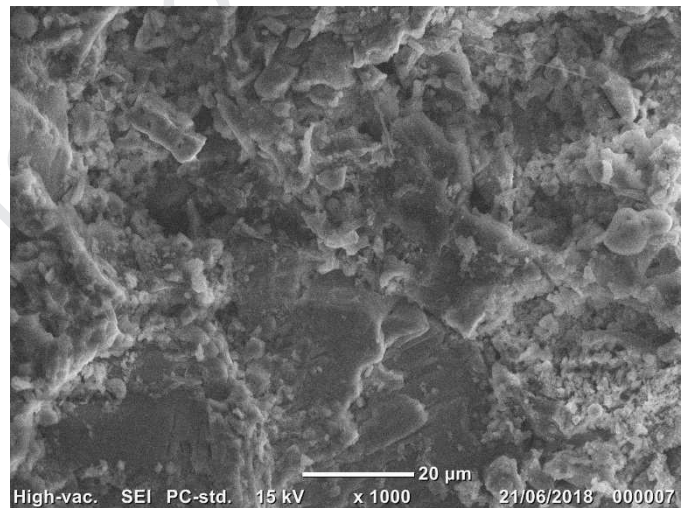
7

525 (a) F0 at room temperature  
526

(b) F0 at 80°C



527



528 (c) F60 at room temperature

(d) F60 at 80°C

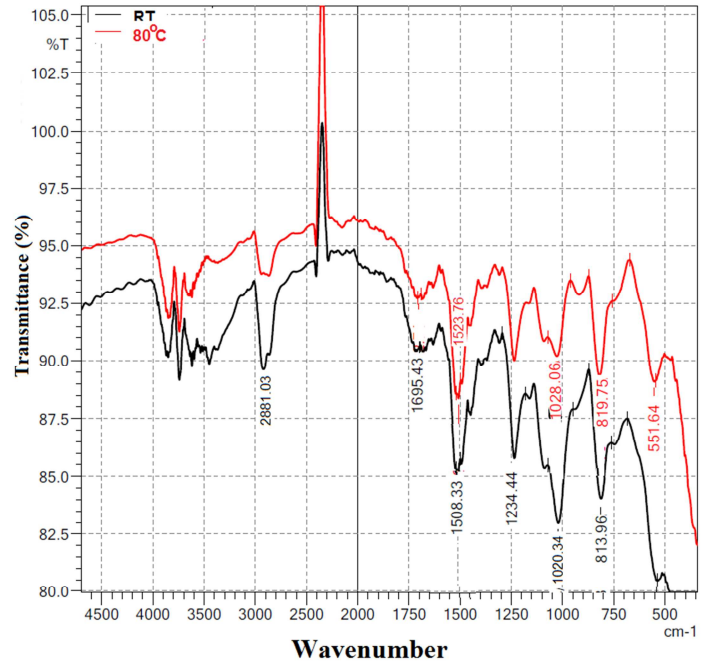
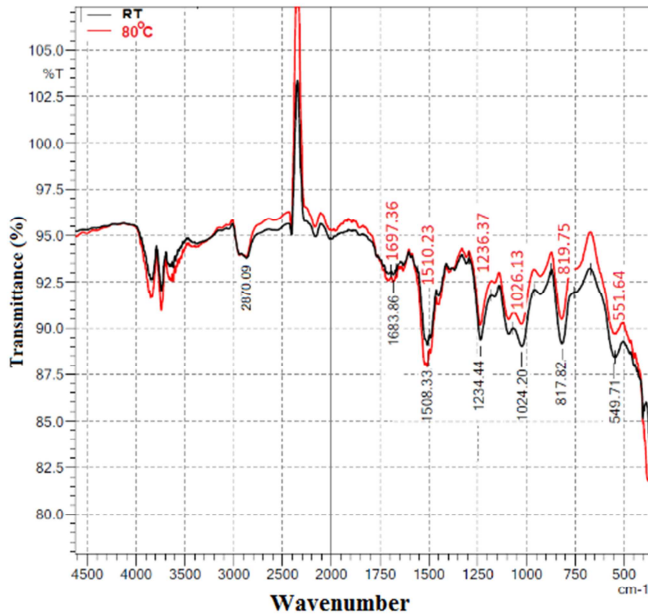
529 **Figure 14: SEM micrographs of particulate filled epoxy resins**

#### 530 **4.6 FTIR results of particulate filled resin subjected to elevated temperature**

531 FTIR spectra was performed after the mechanical tests to determine functional groups  
532 presented in the particulate filled epoxy base resin. The mixing of epoxy resin produced  
533 carboxylic and carbonyl acid by-products due to the reaction of the curing agent and epoxy  
534 resin [51]. The solid particulate-filled epoxy resin composite was formed through the ring  
535 opening polymerisation reaction in the presence of DGEBA, amine-based hardener and fillers  
536 (FA and FR). During the reaction, the carboxyl groups or hydroxyl groups were produced

537 that presented as a pendant in part A. From the spectrum, the characteristic bands of F0, F20,  
538 F40 and F60 were observed at various wavenumbers as shown in **Figure 15**. C-H and C-O  
539 were found to be major phases for all specimens. The band observed at  $\sim 3800\text{ cm}^{-1}$  for  
540 different mixes corresponded to O-H stretching band. The second group of the bands, which  
541 were located at  $2904\text{ cm}^{-1}$  and  $2870\text{ cm}^{-1}$  were attributed to the stretching vibration of C-H  
542 group of epoxy [52, 53]. However, the intensity of these wavenumbers decreased with further  
543 increase of fillers (F40 and F60). Instead of the wavenumber of  $2000\text{ cm}^{-1}$ , the third group of  
544 bands were detected. The band at  $1703\text{ cm}^{-1}$  and  $1718\text{ cm}^{-1}$  was due to the stretching  
545 vibration of C-O in ester [3]. The bands at wavenumber  $1508\text{ cm}^{-1}$  was the characteristic band  
546 for the aromatic ring stretching of C=C, characteristic of DGEBA epoxy systems [54]. The  
547 band at  $1508\text{ cm}^{-1}$  may also represent nitro deformation from the cycloaliphatic amine curing  
548 agent. The bands corresponding to epoxide ring ( $\sim 817\text{ cm}^{-1}$ ) wavenumbers at 1024 and 1234  
549  $\text{cm}^{-1}$  were characteristic bands for C-O stretching of saturated aliphatic primary alcohols [48,  
550 55], unlike the bands observed at C-O for F0 and F20 (resin-rich mixes), where a restrictive  
551 stretching with further inclusion of filler was observed (**Figures 15c and 15d**). This was due  
552 to the decrease in the amount of resin by increasing the percentages of fillers. As shown in  
553 **Figure 15**, mixes of all of the functional groups have the same peak values at their lowest and  
554 highest temperatures except for the shifting bands by increasing the temperatures, particularly  
555 for resin-rich samples (F0 and F20). A small shift of bands to higher wavenumbers by 5 to 15  
556  $\text{cm}^{-1}$  was observed in the spectra with the inclusion of fillers due to the interaction between  
557 epoxy and fillers (FA and FR). FTIR results demonstrate that the curing reaction completed  
558 and the formation of polymeric epoxy structures in all the particulate composites was done.  
559 These results are in accordance with SEM images showing the formation of solid resin after  
560 the curing reaction. (**Figure 14**). These results showed that the sensitivity of epoxy resin  
561 against in-service temperature can be sufficiently reduced by the inclusion of fillers. This

562 further indicates that the particulate filled epoxy resin will exhibit better engineering  
 563 properties against in-service elevated temperature, as the fillers provide protection against  
 564 thermal conditioning increasing their durability and suitability in civil engineering



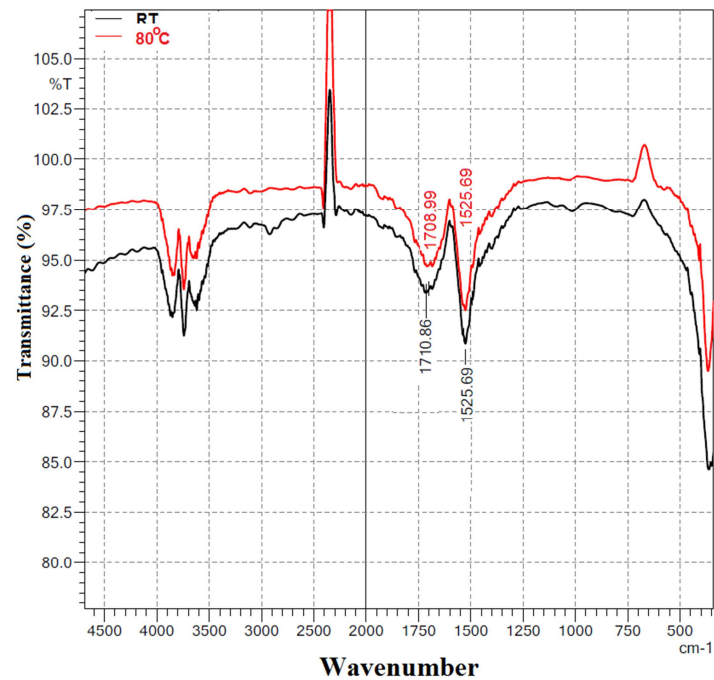
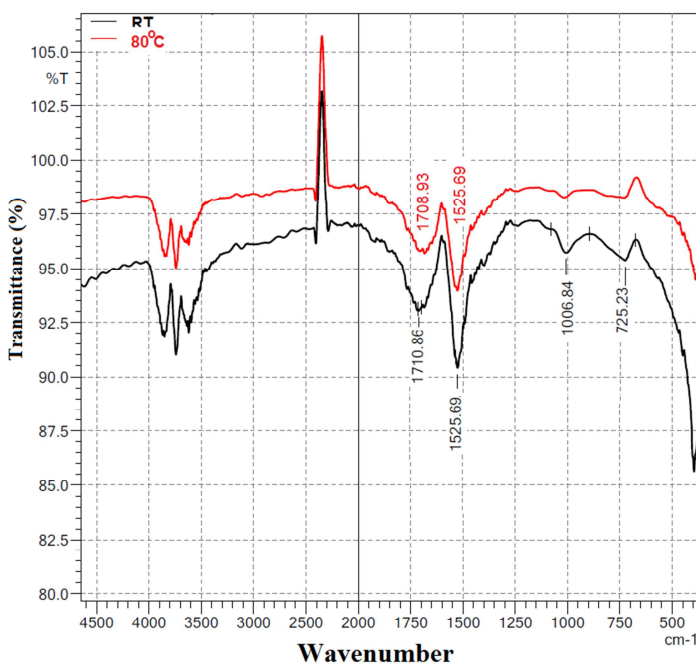
565 applications.

566

567

(a) F0

(b) F20



568

569

(c) F40

(d) F60

570 **Figure 15.** FTIR graphs at room temperature and at 80°C

## 571 **5. Simplified prediction model for particulate-filled epoxy based resin**

572 The results from this study showed that the mechanical properties of particulate-filled epoxy  
 573 resin were very much affected by the in-service temperature while the percentages of fillers  
 574 played a major role in retaining its mechanical properties. This section presents the  
 575 development of a prediction model that describes reliably the mechanical properties of  
 576 particulate-filled epoxy resin with different percentages of fillers and subjected to in-service  
 577 elevated temperature.

### 578 **5.1. Development of prediction model**

579 Saberian et al. [56, 57] and Mohajerani, et al. [58] proposed a power function for predicting  
 580 the resilient modulus of recycled pavement material containing different percentages of fine  
 581 and coarse rubber. In the development of the model, they used the regression coefficients of  
 582 the relationship between the resilient modulus, confining stress, deviator stress, and stiffness  
 583 of recycled pavement mixes from the results of their experimental works. Following this  
 584 approach, in this study, the compressive strength and splitting tensile strength were presented  
 585 as a function of the in-service elevated temperature along with the amount of fillers, to  
 586 estimate the strength of the particulate-filled epoxy resin using a power function. Eq. (2)  
 587 showed the general form to evaluate the relationship between the predicted values (Y),  
 588 mechanical strength, temperature, and percentage fillers.

$$589 \quad Y = K_1 \times (X_1)^{K_2} \times (X_2)^{K_3} \quad (2)$$

590 where  $X_1$  is percentage amount of fillers,  $X_2$  is the level of in-service elevated temperature,  
 591 and  $K_1$ ,  $K_2$ ,  $K_3$  are regression parameters.

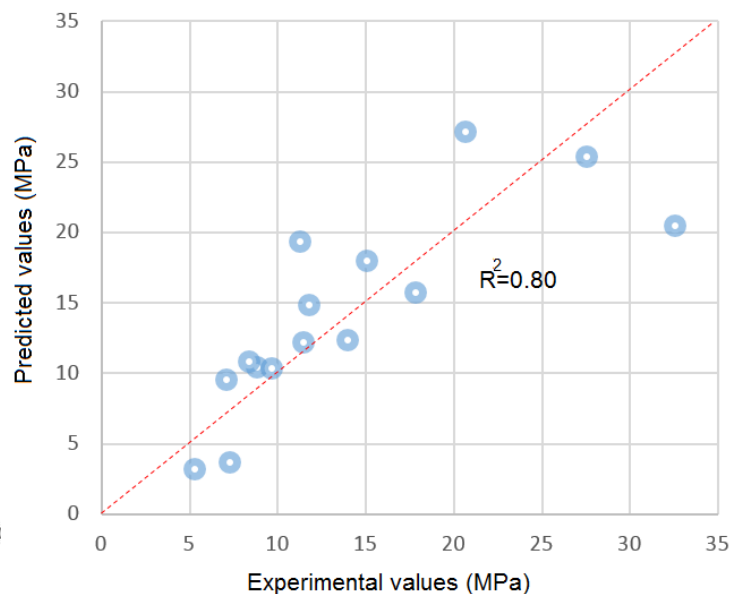
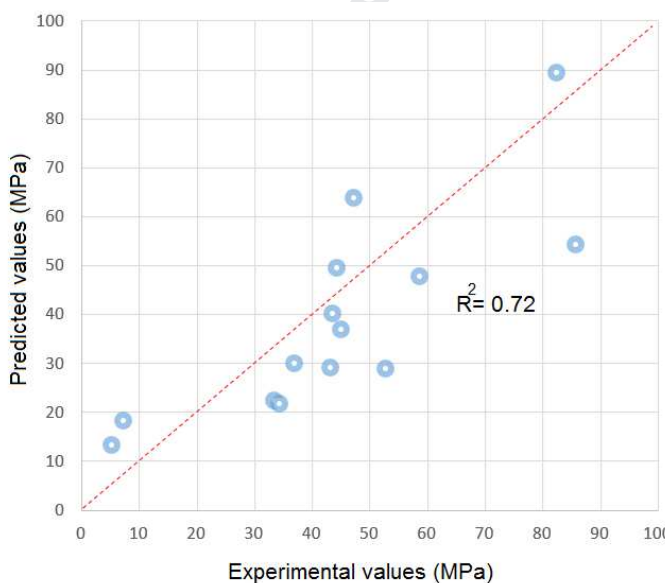
592 The regression equations to predict the compressive strength ( $Y_{Comp}$ ) and the splitting tensile  
 593 strength ( $Y_{Split\_tensile}$ ) are presented in **Table 5**. The regression parameters of the different



594 samples were calculated based on the experimental results fitted against the power function  
 595 model using Excel, where the strength properties, amount of fillers and different levels of  
 596 temperature were given as input. The regression parameters were achieved as product of  
 597 matrix calculations. The coefficient of determination,  $R^2$  for the prediction models has also  
 598 been provided in **Table 5**, while the relationship between the experimental and predicted  
 599 values has been provided in **Figure 16**. In both equations,  $K_1$  and  $K_2$  are positive values,  
 600 implying that the outputs increased with an increase in the amount of filler while  $K_3$  is  
 601 negative indicating that by increasing the temperature, the mechanical properties will  
 602 decrease.

603 **Table 5.** Equations of the prediction model of the particulate-filled epoxy based resin based  
 604 on the relationships among the experimental values, percentages of fillers, and temperature.

Equation	$R^2$
$Y_{Comp} = 222.910 \times (\text{Filler content})^{0.719} \times (\text{Temp})^{-1.1379}$	0.72
$Y_{Split\_tensile} = 183.088 \times (\text{Filler content})^{0.413} \times (\text{Temp})^{-1.090}$	0.80



608 (a)

609

(b)

610

**Figure 16.** Relationship between the experimental and predicted values a) compressive

611

strength and b) splitting tensile strength

612

## 5.2. Correlation between compressive strength and splitting tensile test results

613

The compressive strength test of epoxy-based resin, incorporating different percentages of

614

fillers tested under in-service elevated temperature were presented against splitting tensile

615

strength in **Figure 17** in order to understand the interdependence between these strength

616

properties. It can be observed in the figure that there is a significant linear relationship

617

between the compressive strength and the splitting tensile strength, with the coefficient of

618

correlation of 0.95. This coefficient of correlation is very high and reflects a strong

619

relationship between two different tests. This result also showed that the splitting tensile

620

strength,  $UCS_{Split\_tensile}$  of the particulate-filled epoxy resin with different percentages of

621

fillers and subjected to in-service elevated temperature can be predicted from its compressive

622

strength, which is given as Eq. (2). It is recommended however that the reliability of this

623

proposed equation be validated against percentages of fillers and in-service elevated

624

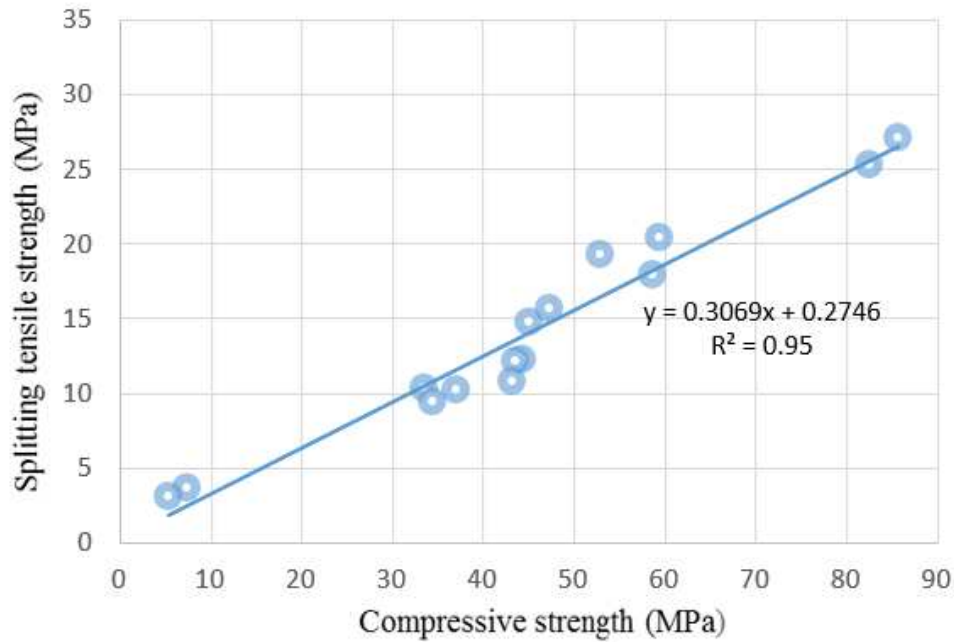
temperature outside the levels investigated in this study.

625

$$Y_{Split\_tensile} = 0.3069(Y_{Comp}) + 0.2746$$

626

(2)



627

628 **Figure 17.** Relationship between the compressive strength and splitting tensile strength629 **5 Conclusions**

630 In this study, the physical, thermo-mechanical, and microstructural properties of epoxy-based  
 631 polymers with different percentages of particulate fillers composed of fly-ash and fire  
 632 retardant fillers were evaluated at elevated temperatures. From the results, the following  
 633 conclusions are drawn:

- 634 • The density of particulate-filled epoxy-based polymer resin increased with increasing  
 635 amount of fillers. However, a higher discrepancy between the actual and calculated  
 636 densities was noted for mixes with higher amount of fillers than those with lower  
 637 amount of fillers due to an increase in the amount and size of pores in these samples.
- 638 • The size and number of pores of the particulate-filled epoxy-based polymer resin  
 639 decreased with increasing temperature due to softening of the epoxy resin.
- 640 • Thermo-dynamical analysis from DMA test showed that adding 0–60% of filler to the  
 641 polymer matrix could increase the  $T_g$  by at least  $5^\circ\text{C}$ . Furthermore, results of SDT

642 showed that the thermal stability of epoxy-based resin at high temperatures was  
643 improved by the inclusion of FA and FR.

- 644 • Large increases in ductility (strain to failure) and reduction in ultimate strength were  
645 observed at elevated temperatures. Nevertheless, the addition of fillers led to retention  
646 of compressive and tensile strengths by up to 72% and 52%, respectively for F60 at  
647 the maximum test temperature of 80°C. This high mechanical strength retention was  
648 due to the high thermal stability of particulate fillers.
- 649 • SEM images showed the formation of dense microstructure with utilizing fillers in the  
650 mixtures at high temperatures. This resulted in higher compressive and split tensile  
651 strength retention in epoxy with fillers under elevated temperature.
- 652 • FTIR analysis indicated that C-H and C-O were found to be major phases for all  
653 specimens. However, there was restrictive stretching with the addition of filler up to  
654 60%. The curing reaction was completed and the formation of polymeric epoxy  
655 structures in all the particulate-filled resins was performed. All of the functional group  
656 mixes had the same peak values at their lowest and highest temperatures and except  
657 for shifting of band by increasing of temperatures, particularly for resin-rich samples,  
658 which shows the in-service temperature, did not lead to significant changes in the  
659 spectra of different mixes.
- 660 • A simplified prediction equation based on power function was developed to predict  
661 the mechanical properties of the epoxy resin system with different percentages of  
662 particulate fillers at in-service elevated temperatures. Comparison between the  
663 predicted values and experimental results showed a strong correlation and the  
664 coefficient of correlation is at least 0.72.

665 The above results showed that the sensitivity of epoxy resin against in-service  
666 temperatures can be significantly improved by the inclusion of particulate fillers. This

667 type of polymer matrix is suitable for manufacturing infrastructures exposed to the  
668 environment such as polymer railway sleepers, chemical storage tanks, and bridge  
669 girders. Continued efforts should be made towards understanding the behaviour of these  
670 new materials when exposed to other environmental factors such as moisture and  
671 photochemical reactions from solar ultraviolet (UV) and their synergetic effect in the  
672 presence of in-service temperatures.

### 673 **Acknowledgements**

674 The first author gratefully acknowledges the financial support including a stipend research  
675 scholarship and fees for a research scholarship from the University of Southern Queensland  
676 for conducting her PhD. The authors also in very thankful to Dr Barbara Harmes for her help  
677 in editing the manuscript. The authors also acknowledge the material support of ATL  
678 Composites Pty Ltd (Gold coast, Australia).

679

### 680 **References:**

- 681 [1] Ferdous, W., Ngo, T.D., Nguyen, K.T., Ghazlan, A., Mendis, P. and Manalo, A.,  
682 2018. Effect of fire-retardant ceram powder on the properties of phenolic-based GFRP  
683 composites. *Composites Part B: Engineering*, 155, pp.414-424.
- 684 [2] Cantwell, W.J., Roulin-Moloney, A.C. and Kaiser, T., 1988. Fractography of unfilled  
685 and particulate-filled epoxy resins. *Journal of materials science*, 23(5), pp.1615-1631.
- 686 [3] Yang, Y., Xian, G., Li, H. and Sui, L., 2015. Thermal aging of an anhydride-cured  
687 epoxy resin. *Polymer degradation and stability*, 118, pp.111-119.
- 688 [4] Jia, P., Liu, H., Liu, Q. and Cai, X., 2016. Thermal degradation mechanism and flame  
689 retardancy of MQ silicone/epoxy resin composites. *Polymer Degradation and*  
690 *Stability*, 134, pp.144-150.
- 691 [5] Strong, A. B. 2008. *Fundamentals of composites manufacturing: materials, methods*  
692 *and applications*, Society of Manufacturing Engineers.
- 693 [6] Issa, C. A. & Debs, P. 2007. Experimental study of epoxy repairing of cracks in  
694 concrete. *Construction and Building Materials*, 21, 157-163
- 695 [7] Michels, J., Widmann, R., Czaderski, C., Allahvirdizadeh, R. and Motavalli, M.,  
696 2015. Glass transition evaluation of commercially available epoxy resins used for  
697 civil engineering applications. *Composites Part B: Engineering*, 77, pp.484-493.
- 698 [8] Manalo, A.C., Surendar, S., van Erp, G., and Benmokrane, B. (2016). Flexural  
699 behavior of an FRP sandwich system with glass-fiber skins and a phenolic core at  
700 elevated in-service temperature. *Composite Structures*, 152: 96-105.

- 701 [9] Ferdous, W., Manalo, A., Aravinthan, T. & Van Erp, G. 2016. Properties of epoxy  
702 polymer concrete matrix: Effect of resin-to-filler ratio and determination of optimal  
703 mix for composite railway sleepers. *Construction and Building Materials*, 124, 287-  
704 300.
- 705 [10] Duell, J., Wilson, J. & KESSLER, M. 2008. Analysis of a carbon composite  
706 overwrap pipeline repair system. *International Journal of Pressure Vessels and Piping*,  
707 85, 782-788.
- 708 [11] Azraai, S., Lim, K., Yahaya, N. & Noor, N. 2015. Infill materials of epoxy  
709 grout for pipeline rehabilitation and repair. *Malaysian Journal of Civil Engineering*,  
710 27, 162-167.
- 711 [12] Shamsuddoha, M., Islam, M.M., Aravinthan, T., Manalo, A. and Lau, K.T.,  
712 2013. Effectiveness of using fibre-reinforced polymer composites for underwater steel  
713 pipeline repairs. *Composite Structures*, 100, pp.40-54.
- 714 [13] Mohammed, A.A., Manalo, A.C., Maranan, G.B., Zhuge, Y. and Vijay, P.V.,  
715 2018. Comparative study on the behaviour of different infill materials for pre-  
716 fabricated fibre composite repair systems. *Construction and Building Materials*, 172,  
717 pp.770-780.
- 718 [14] Ferdous, W., Manalo, A. and Aravinthan, T., 2017. Bond behaviour of  
719 composite sandwich panel and epoxy polymer matrix: Taguchi design of experiments  
720 and theoretical predictions. *Construction and Building Materials*, 145, pp.76-87.
- 721 [15] Sirimanna, C., Islam, M.M., Aravinthan, T. Temperature effects on full scale  
722 FRP bridge using innovative composite components. *Advances in FRP Composites in*  
723 *Civil Engineering*. Springer, 2011, 376-380.
- 724 [16] Manalo, A.C., Maranan, G., Sharma, S., Karunasena, W., and Bai, Y. (2017).  
725 Temperature-sensitive mechanical properties of GFRP composites in longitudinal and  
726 transverse directions: A comparative study. *Composite Structures*, 173, 255–267.
- 727 [17] Anderson, B.J., 2011. Thermal stability of high temperature epoxy adhesives  
728 by thermogravimetric and adhesive strength measurements. *Polymer degradation and*  
729 *stability*, 96(10), pp.1874-1881.
- 730 [18] Polanský, R., Mentlík, V., Prosr, P. and Sušír, J., 2009. Influence of thermal  
731 treatment on the glass transition temperature of thermosetting epoxy laminate.  
732 *Polymer Testing*, 28(4), pp.428-436.
- 733 [19] Anderson, B.J., 2013. Thermal stability and lifetime estimates of a high  
734 temperature epoxy by Tg reduction. *Polymer degradation and stability*, 98(11),  
735 pp.2375-2382.
- 736 [20] Koh, S.W., Kim, J.K. and Mai, Y.W., 1993. Fracture toughness and failure  
737 mechanisms in silica-filled epoxy resin composites: effects of temperature and  
738 loading rate. *Polymer*, 34(16), pp.3446-3455.
- 739 [21] Fu, S.Y., Feng, X.Q., Lauke, B. and Mai, Y.W., 2008. Effects of particle size,  
740 particle/matrix interface adhesion and particle loading on mechanical properties of  
741 particulate–polymer composites. *Composites Part B: Engineering*, 39(6), pp.933-961.
- 742 [22] Karbhari, V.M., 2007. Fabrication, quality and service-life issues for  
743 composites in civil engineering. In *Durability of composites for civil structural*  
744 *applications* (pp. 13-30).

- 745 [23] Ray, B.C., 2006. Temperature effect during humid ageing on interfaces of  
746 glass and carbon fibers reinforced epoxy composites. *Journal of Colloid and Interface*  
747 *Science*, 298(1), pp.111-117.
- 748 [24] Mauerer, O., 2005. New reactive, halogen-free flame retardant system for  
749 epoxy resins. *Polymer Degradation and Stability*, 88(1), pp.70-73.
- 750 [25] Wang, P., Xia, L., Jian, R., Ai, Y., Zheng, X., Chen, G. and Wang, J., 2018.  
751 Flame-retarding epoxy resin with an efficient P/N/S-containing flame retardant:  
752 preparation, thermal stability, and flame retardance. *Polymer Degradation and*  
753 *Stability*, 149, pp.69-77.
- 754 [26] Khotbehsara, M.M., Mohseni, E., Yazdi, M.A., Sarker, P. and Ranjbar, M.M.,  
755 2015. Effect of nano-CuO and fly ash on the properties of self-compacting mortar.  
756 *Construction and Building Materials*, 94, pp.758-766.
- 757 [27] Khotbehsara, M.M., Miyandehi, B.M., Naseri, F., Ozbakkaloglu, T., Jafari, F.  
758 and Mohseni, E., 2018. Effect of SnO<sub>2</sub>, ZrO<sub>2</sub>, and CaCO<sub>3</sub> nanoparticles on water  
759 transport and durability properties of self-compacting mortar containing fly ash:  
760 Experimental observations and ANFIS predictions. *Construction and Building*  
761 *Materials*, 158, pp.823-834.
- 762 [28] Moloney, A.C., Kausch, H.H., Kaiser, T. and Beer, H.R., 1987. Parameters  
763 determining the strength and toughness of particulate filled epoxide resins. *Journal of*  
764 *materials science*, 22(2), pp.381-393.
- 765 [29] Bărbuță, M., Harja, M. & Baran, I. 2009. Comparison of mechanical  
766 properties for polymer concrete with different types of filler. *Journal of Materials in*  
767 *Civil Engineering*, 22, 696-701.
- 768 [30] Rebeiz, K., Serhal, S. & Craft, A. 2004. Properties of polymer concrete using  
769 fly ash. *Journal of Materials in Civil Engineering*, 16, 15-19
- 770 [31] Gorninski, J. P., Dal Molin, D. C. & Kazmierczak, C. S. 2004. Study of the  
771 modulus of elasticity of polymer concrete compounds and comparative assessment of  
772 polymer concrete and portland cement concrete. *Cement and Concrete Research*, 34,  
773 2091-2095.
- 774 [32] Lokuge, W. & Aravinthan, T. 2013. Effect of fly ash on the behaviour of  
775 polymer concrete with different types of resin. *Materials & Design*, 51, 175-181.
- 776 [33] W. Ferdous, A. Manalo, G. Van Erp, T. Aravinthan, K. Ghabraie, Evaluation  
777 of an innovative composite railway sleeper for a narrow-gauge track under static load,  
778 *Journal of Composites for Construction* 22(2) (2018) 1-13.
- 779 [34] W. Ferdous, A. Manalo, T. Aravinthan, A. Fam, Flexural and shear behaviour  
780 of layered sandwich beams, *Construction and Building Materials* 173 (2018) 429-442.
- 781 [35] ASTM Standard, ASTM C905: Standard Test Methods for Apparent Density  
782 of Chemical Resistant Mortars, Grouts, Monolithic Surfacing, and Polymer  
783 Concretes, United States, 2012.
- 784 [36] ASTM Standard, ASTM D7028: Standard Test Method for Glass Transition  
785 Temperature (DMA T<sub>g</sub>) of Polymer Matrix Composites by Dynamic Mechanical  
786 Analysis (DMA), United States, 2008.
- 787 [37] Etaati, A., Pather, S., Fang, Z. and Wang, H., 2014. The study of fibre/matrix  
788 bond strength in short hemp polypropylene composites from dynamic mechanical  
789 analysis. *Composites Part B: Engineering*, 62, pp.19-28.



- 790 [38] ASTM Standard, ASTM C579: Standard Test Methods for Compressive  
791 Strength of Chemical-Resistant Mortars, Grouts, Monolithic Surfacing, and Polymer  
792 Concretes, United States, 2012.
- 793 [39] Viklund, C., Svec, F., Fréchet, J.M. and Irgum, K., 1996.  
794 Monolithic, “molded”, porous materials with high flow characteristics for separations,  
795 catalysis, or solid-phase chemistry: control of porous properties during  
796 polymerization. *Chemistry of materials*, 8(3), pp.744-750.
- 797 [40] Lin, C. and Ritter, J.A., 2000. Carbonization and activation of sol-gel derived  
798 carbon xerogels. *Carbon*, 38(6), pp.849-861.
- 799 [41] Ashrafi, H., Bazli, M., Vatani Oskouei, A. and Bazli, L., 2017. Effect of  
800 Sequential Exposure to UV Radiation and Water Vapor Condensation and Extreme  
801 Temperatures on the Mechanical Properties of GFRP Bars. *Journal of Composites for*  
802 *Construction*, 22(1), p.04017047.
- 803 [42] Shamsuddoha, M., Islam, M.M., Aravinthan, T., Manalo, A. and Lau, K.T.,  
804 2013. Characterisation of mechanical and thermal properties of epoxy grouts for  
805 composite repair of steel pipelines. *Materials & Design (1980-2015)*, 52, pp.315-327.
- 806 [43] Aghadavoudi, F., Golestanian, H. and Tadi Beni, Y., 2017. Investigating the  
807 effects of resin crosslinking ratio on mechanical properties of epoxy-based  
808 nanocomposites using molecular dynamics. *Polymer Composites*, 38, pp.E433-E442.
- 809 [44] Jiang, H., Su, W., Mather, P.T. and Bunning, T.J., 1999. Rheology of highly  
810 swollen chitosan/polyacrylate hydrogels. *Polymer*, 40(16), pp.4593-4602.
- 811 [45] Liu, R. and Wang, X., 2009. Synthesis, characterization, thermal properties  
812 and flame retardancy of a novel nonflammable phosphazene-based epoxy  
813 resin. *Polymer degradation and stability*, 94(4), pp.617-624.
- 814 [46] Preghenella, M., Pegoretti, A. and Migliaresi, C., 2005. Thermo-mechanical  
815 characterization of fumed silica-epoxy nanocomposites. *Polymer*, 46(26), pp.12065-  
816 12072.
- 817 [47] Bajracharya, R.M., Manalo, A.C., Karunasena, W., and Lau, K.T.  
818 (2017). Durability characteristics and property prediction of glass fibre reinforced  
819 mixed plastics composites. *Composites Part B: Engineering*, 116, 16–29
- 820 [48] Goyanes, S.N., König, P.G. and Marconi, J.D., 2003. Dynamic mechanical  
821 analysis of particulate-filled epoxy resin. *Journal of applied polymer science*, 88(4),  
822 pp.883-892.
- 823 [49] Kenyon, A.S. and Duffey, H.J., 1967. Properties of a particulate-filled  
824 polymer. *Polymer Engineering & Science*, 7(3), pp.189-193.
- 825 [50] Ahmad, F.N., Jaafar, M., Palaniandy, S. and Azizli, K.A.M., 2008. Effect of  
826 particle shape of silica mineral on the properties of epoxy composites. *Composites*  
827 *Science and Technology*, 68(2), pp.346-353.
- 828 [51] Tcherbi-Narteh, A., Hosur, M., Triggs, E. and Jeelani, S., 2013. Thermal  
829 stability and degradation of diglycidyl ether of bisphenol A epoxy modified with  
830 different nanoclays exposed to UV radiation. *Polymer degradation and*  
831 *stability*, 98(3), pp.759-770.
- 832 [52] Noobut, W. and Koenig, J. L., 1999. Interfacial behavior of epoxy/E-glass  
833 fiber composites under wet-dry cycles by fourier transform infrared  
834 microspectroscopy. *Polymer composites*, 20(1), pp.38-47.



- 835 [53] Wang, Z., Zhao, X.L., Xian, G., Wu, G., Raman, R.S. and Al-Saadi, S., 2017.  
836 Durability study on interlaminar shear behaviour of basalt-, glass-and carbon-fibre  
837 reinforced polymer (B/G/CFRP) bars in seawater sea sand concrete  
838 environment. *Construction and Building Materials*, 156, pp.985-1004.Y.M.
- 839 [54] Cherdoud-Chihani, A., Mouzali, M. and Abadie, M.J.M., 2003. Study of  
840 crosslinking acid copolymer/DGEBA systems by FTIR. *Journal of applied polymer  
841 science*, 87(13), pp.2033-2051.
- 842 [55] Delor-Jestin, F., Drouin, D., Cheval, P.Y. and Lacoste, J., 2006. Thermal and  
843 photochemical ageing of epoxy resin–Influence of curing agents. *Polymer  
844 Degradation and Stability*, 91(6), pp.1247-1255.
- 845 [56] Saberian, M., Li, J., Nguyen, B.T. and Setunge, S., 2019. Estimating the  
846 resilient modulus of crushed recycled pavement materials containing crumb rubber  
847 using the Clegg impact value. *Resources, Conservation and Recycling*, 141, pp.301-  
848 307.
- 849 [57] Saberian, M., Shi, L., Sidiq, A., Li, J., Setunge, S. and Li, C.Q., 2019.  
850 Recycled concrete aggregate mixed with crumb rubber under elevated temperature.  
851 *Construction and Building Materials*, 222, pp.119-129.
- 852 [58] Mohajerani, A., Nguyen, B., Glavacevic, L., 2016. Estimation of resilient  
853 modulus of  
854  
855  
856

### **Highlights**

- Degradation and stability of particulate-filled epoxy polymers at elevated temperature.
- High strength retention of epoxy due to the high thermal stability of fillers.
- Fillers make epoxy resin with a dense microstructure at elevated temperature.
- FTIR analysis revealed no chemical changes in the epoxy at elevated temperature.
- Strong correlation between predicted values and experimental results